4. Fusion Confinement

The attainment of a sufficiently high reaction-driven energy density is a requirement of all energy systems. For fusion it is essential that the reactant nuclei attain a sufficiently high kinetic energy of relative motion in order to achieve substantial rates of exothermic reactions. These conditions must then be retained for a sufficiently long time in a specified reaction domain. Confining the interacting fuel particles at an appropriate high temperature is thus a most basic consideration of fusion energy systems.

4.1 Necessity of Confinement

Unlike fission reactions which involve a neutral reactant and thus do not experience repulsive effects, fusion reactants are positively charged and must overcome their electrostatic repulsion in order to get close enough for the strong nuclear forces of attraction to dominate. Hence, the essential condition for fusion is the requirement for a sufficiently high kinetic temperature of the reacting species in order to facilitate the penetration of the Coulomb barrier.

The attainment of ion energies in excess of this Coulomb barrier, which is about 370 keV for d-t fusion, poses little technical difficulty. For example, readily available medium-energy accelerators could be used to inject deuterons, of say $E_d \approx 500$ keV, into a tritiated target; surrounding neutron and alpha detectors could then be used to identify the reaction products as evidence of whether the reaction $d + t \rightarrow n + \alpha + 17.6$ MeV had taken place. Obviously, if each injected deuteron were to lead to d-t fusion, then the energy multiplication would be $E_{out} / E_{in} = 17.6 / 0.5 = 35$ and thus adequate for fusion energy utility purposes.

Theory suggests and experiment has confirmed that such a beam-target concept is totally inadequate for the following reasons: as beam deuterons enter a target they lose energy through the processes of ionization and heating the target. As discussed in the preceding chapter and displayed in Fig. 3.5, they are far more likely to scatter–rather than fuse–with an additional attendant energy loss by bremsstrahlung radiation. Thus, very quickly, the projectiles will have slowed down to energies far below the Coulomb barrier rendering further fusion reactions most unlikely. Thus, the overall fusion energy release can not exceed the energy required for beam acceleration. The futility of this approach was

recognized early in fusion energy research.

A more promising approach, however, soon emerged. One begins with a population of deuterium and tritium atoms in some confined space, and by heating one causes both ionization and the attainment of high temperature of the fuel ions. The resulting ensemble of positive and negative charges thus forms a plasma which is expected to attain thermodynamic equilibrium as a result of random collisions. The resultant spectrum of particle energies is then well described by a Maxwell-Boltzmann distribution with the high energy part of this distribution providing for most of the desired fusion reactions. Because the reaction activation occurs here due to random thermal motion of the reacting nuclei, this process is therefore called thermonuclear fusion. The critical technical requirement is the sustainment of a sufficiently stable high temperature ($\sim 10^8$ K) plasma in a practical reaction volume and for a sufficiently long period of time to render the entire process energetically viable. Confinement of the fuel ions by some means is thus crucial to maintain these conditions within the required reaction volume.

We add that in contrast to this high-temperature approach to fusion, there exists also a low-temperature approach free of the above type of confinement problems. As we will show in Ch. 12, confinement by atomic-molecular effects may also be exploited.

4.2 Material Confinement

The simplest and most obvious method with which to provide confinement of a plasma is by a direct-contact with material walls, but is impossible for two fundamental reasons: the wall would cool the plasma and most wall materials would melt. We recall that the fusion plasma here requires a temperature of $\sim 10^8$ K while metals generally melt at a temperature below 5000 K.

Further, even for a plasma not in direct contact, there exist problems with a material wall. High temperature particles escaping from the plasma may strike the wall causing so-called "sputtered" wall atoms to enter the plasma. These particles will quickly become ionized by collisions with the background plasma and can appear as multiply-charged ions which are known as fusion plasma impurities. Then, as shown in the analysis leading to Eq. (3.44), the bremsstrahlung power losses increase with Z^2 thus further cooling the plasma.

4.3 Gravitational Confinement

A most spectacular display of fusion energy is associated with stars, where confinement comes about because of the gravitational pressure of an enormous mass. High density and temperature thereby result toward the stellar centre

enabling the fusile ions to burn. While energy leakage and particle escape occurs from the star's surface, the interior retains most of the reaction power and prevails against the occurrent radiation pressure through the deep gravitational potential wells, thus assuring stable confinement for times long enough to burn most of the stellar fusionable inventory.

Since fusion-powered stars possess dimensions and masses of such enormity , it is evident that confinement by gravity cannot be attained in our terrestrial environment.

4.4 Electrostatic Confinement

A more plausible approach to the confinement problem is to recognize that ions are known to be affected by electrostatic fields, so that confinement by such force effects can also be conceived.

One specific and interesting electrostatic approach to confinement involves a spherical metallic anode emitting deuterons towards the centre. These ions then pass through a spherical negatively charged grid designed to be largely transparent to these deuterons. The positive ions converge toward the centre and a positive space charge forms tending to reverse the motion of the ions and thereby establish a positive ion shell inside the hollow cathode. This internal positive ion shell is called a "virtual anode" in order to distinguish it from the "real anode" which produced these ions.

The metallic cathode, situated between the real and virtual anode, also emits electrons towards the centre. After passage through the virtual anode, the electrons similarly form a "virtual cathode" located further towards the centre. It is conceived that several such nested virtual cathodes and virtual anodes will form with the ion density increasing toward the centre. Finally, then, fusion reactions are expected to occur in these inner ion shells of increasing particle density.

However, in general, the electric fields required, the likelihood of discharge breakdown, and problems of geometrical restrictions have generally served to limit consideration of electrostatic confinement in the pursuit of fusion reaction rates suitable for an energetically viable system.

4.5 Inertial Confinement

A confinement method with apparently more merit than the aforementioned is inertial confinement fusion, involving compression of a small fusion fuel pellet to high density and temperature by external laser or ion beams, Fig.4.1. The density-temperature conditions so achieved are expected to provide for a pulse of fusion energy before pellet disassembly. The incident laser or ion beam induces an

inward directed momentum of the outer layers of the pellet, thereby yielding a high density of material, the inertia of which confines the fuel against the fusion reaction explosive effect of disassembly for a sufficient time to allow enough fusion reactions to occur.

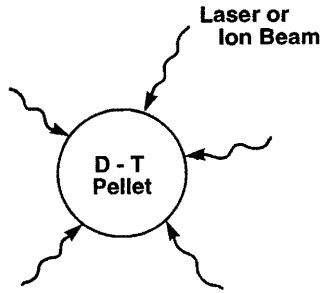

Fig. 4.1: Compression and heating of a d-t pellet by external laser or ion beams.

Some critical characteristic features of inertially confined fusion can be described by the following. Consider, for this purpose, a d-t pellet at an advanced stage of compression with a plasma formed therefrom and fusion burn occurring. The tritium ion density N_t will, in the absence of leakage, decrease according to its burn rate

$$\frac{dN_t}{dt} = -<\sigma v>_{dt} N_d N_t \qquad (4.1)$$

with the symbols here used as previously defined. In this context, we may further identify a triton mean-life, τ_t, by

$$\frac{dN_t}{dt} = -\frac{N_t}{\tau_t} . \qquad (4.2)$$

This triton mean-life may evidently be identified as the mean time between fusion events, τ_{fu}, which by equating Eq.(4.1) with (4.2), yields specifically

$$\tau_{fu} \approx \frac{1}{<\sigma v>_{dt} N_{d,o}} \qquad (4.3)$$

with $N_d = N_{d,o}$ taken to be some suitable initial average deuterium population density and $<\sigma v>_{dt}$ is taken at some appropriate average temperature. Expecting the pellet disassembly to be rapid suggests that τ_{fu} should also be small. Two possibilities of reducing τ_{fu} become evident from Eq.(4.3). One can enhance $<\sigma v>$ by increasing the relative speed of the reactants which, however, is limited by the techniques of heat deposition in the fuel as well as by the more rapid disintegration at higher temperatures. The other option is to increase the fuel

density by several orders of magnitude. The reaction rate parameter $<\sigma v>_{dt}$ is a maximum at an ion temperature of ~60 keV, and the density is a maximum at the onset of fusion burn which is also occurring at the time pellet disassembly begins.

A pellet, once compressed and with fusion reactions taking place, will evidently heat up further and hence tend toward disintegration. The speed of outward motion of the pellet atoms is, to a first approximation, given by the sonic speed v_s which, in a d-t plasma, is given by

$$v_s = \sqrt{\gamma \frac{2N_i kT}{N_i \overline{m_i}}} = \sqrt{\frac{10}{3}\frac{kT_i}{\overline{m_i}}} . \qquad (4.4)$$

Here, γ is the ratio of specific heats ($\gamma = 5/3$), N_i is the ion density, and $\overline{m_i}$ the average ion mass.

As a characteristic expansion, we take the pellet's spherical inflation from its initial radius R_b when the fusion burn began, to a size of radius $2R_b$. During this process, the fuel density will have decreased by a factor of 2^3 and the rate of fusion energy release will have accordingly decreased by the factor $(2^3)^2 = 64$; hence, most of the fusion reactions will have taken place during this initial stage of disassembly. Thus, the time for doubling of the pellet radius is taken as being representative of the inertial confinement time, τ_{ic}, given by

$$\tau_{ic} = \frac{2R_b - R_b}{v_s} = R_b \left(\frac{3\overline{m_i}}{10kT_i}\right)^{1/2} . \qquad (4.5)$$

Evidently, τ_{fu} of Eq.(4.3) should be shorter than–or perhaps of the order of–τ_{ic} for sufficient fusion burn to take place so that, as a required initial condition, we must have

$$\tau_{fu} < \tau_{ic} , \qquad (4.6a)$$

that is,

$$\frac{1}{<\sigma v>_{dt} N_{d,o}} < R_b \left(\frac{3\overline{m_i}}{10kT_i}\right)^{1/2} . \qquad (4.6b)$$

For the case of $N_{d,o} = N_{t,o} = N_{i,o}/2$, that is half of the compressed fuel density at the beginning of the fusion burn, we may therefore write the requirement as

$$N_{i,o} R_b > \frac{\left(\frac{40kT_i}{3\overline{m_i}}\right)^{1/2}}{<\sigma v>_{dt}} . \qquad (4.7)$$

Taking an average fusion fuel temperature of about $E_{th} \approx 20$ keV, we obtain by substitution,

$$N_{i,o} R_b > 10^{24} \text{ cm}^{-2} . \qquad (4.8)$$

Some essential technical features of inertial confinement fusion may now be

qualitatively and quantitatively established. First, as will be shown in Ch. 11, the beam energy required to compress a pellet corresponds to the resultant heat content of the compressed pellet, and hence varies as R_b^3. Existing laser beam powers are such that R_b needs to be kept in the range of millimetres or less. Second, the fuel density will evidently need to become very large, typically exceeding 10^3 times that of its equivalent solid density. Finally, the quantity of the initial fuel which burns up needs to be carefully specified since it relates to the overall energy viability of each fusion pulse as well as to the capacity of the surrounding medium to absorb the blast energy.

Thus, as an initial conclusion, we may assert that very high power drivers and very high compression is required for fusion energy achievement by inertial confinement. Further analysis of inertial confinement fusion is the subject of Ch. 11.

4.6 Magnetic Confinement

One of the most effective means of plasma confinement to date involves the use of magnetic fields. A particle of charge q and mass m located in a magnetic field of local flux density **B** is constrained to move according to the Lorentz force given by

$$m\frac{d\mathbf{v}}{dt} = q(\mathbf{v}\times\mathbf{B}) \tag{4.9}$$

with **v** the velocity vector.

For the case of a solenoidal **B**-field produced by a helical electrical current with density **j**, Fig. 4.2a, ions and electrons will move (as will be shown in Ch. 5)–depending upon the initial particle velocity–either parallel or antiparallel to the **B**-field lines and spiral about them with a radius of gyro-motion of

$$r_g \propto \frac{1}{|\mathbf{B}|}\,. \tag{4.10}$$

Scattering reactions may, however, transport them out of these uniform spiral orbits with two consequences: they may be captured into another spiral orbit or they may scatter out of the magnetic field domain. In the absence of scattering they are essentially confined as far as directions perpendicular to **B** are concerned, traveling helically along **B** with an unaffected velocity component parallel to **B**. Subsequently, they will eventually depart from the region of interest.

Solenoidal fields belong to the oldest and most widely used magnetic confinement devices used in plasma physics research. The ion and electron densities may clearly be enhanced by increasing the magnetic field thereby also providing for a smaller radius of gyration. There exists, however, a dominant property which renders their use for fusion energy purposes most detrimental: for

solenoidal dimensions and magnetic fields generally achievable, fuel ion leakage through the ends is so great that these devices provide little prospect for use as fusion reactors.

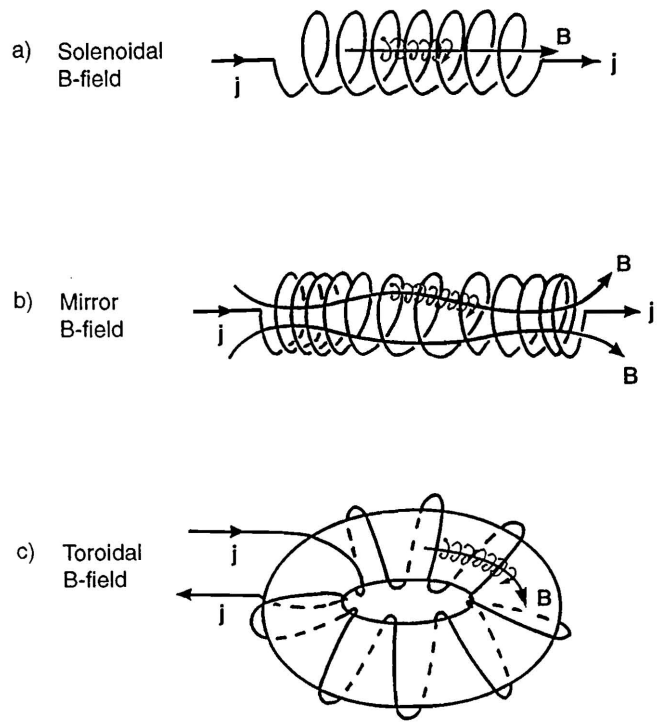

Fig. 4.2: Depiction of three magnetic field topologies and illustrative ion trajectories.

If, however, the magnetic field strength is increased specifically at each end of the cylindrical region, i.e. the **B**-field lines appear to be substantially squeezed together at the ends, Fig. 4.2b, the number of leaking particles is considerably reduced. Such a squeezed field configuration is referred to as a magnetic mirror since it is able to reflect charged particles, as will be shown in Sec. 9.3. We note that ions and electrons possessing excessive motion along the magnetic axis will still penetrate the magnetic mirror throat.

The attractiveness of the mirror concept not withstanding, a magnetic mirror can thus not provide complete confinement and–as in all open-ended configurations–is associated with unacceptably high particle losses through the ends. Hence, to avoid end-leakage entirely, the obvious solution is to eliminate

the ends by turning a solenoidal field into a toroidal field, Fig. 4.2c. The resultant toroidal magnetic field topology has spawned several important fusion reactor concepts; the most widely pursued of such devices is known as the tokamak, which will be discussed in Ch. 10.

At first consideration, the charged particles could be viewed as simply spiraling around the circular field lines in Fig. 4.2c, not encountering an end through which to escape. Any losses would have to occur by scattering or diffusion across field lines in the radial direction causing leakage across the outer surface. Further, we mention that collective particle oscillations may occur, thereby destabilizing the plasma.

One important plasma confinement indicator is the ratio of kinetic particle pressure

$$p_{kin} = N_i kT_i + N_e kT_e \tag{4.11a}$$

to the magnetic pressure

$$p_{mag} = \frac{B^2}{2\mu_o} \tag{4.11b}$$

with μ_o the permeability of free space. This ratio is defined as the beta parameter, β, and is a measure of how effectively the magnetic field constrains the thermal motion of the plasma particles. A high beta would be most desirable but it is also known that there exists a system-specific β_{max} at which plasma oscillations start to destroy the confinement. That is, for confinement purposes, we require

$$\beta_{max} \frac{B^2}{2\mu_o} \geq N_i kT_i + N_e kT_e \ . \tag{4.12}$$

Thus, the maximum plasma pressure is determined by available magnetic fields thereby introducing magnetic field technology as a limit on plasma confinement in toroids.

In order to assess the fusion energy production possible in such a magnetically confined, pressure-limited deuterium-tritium plasma, we introduce Eq.(4.12), with the equality sign, into the fusion power density expression

$$P_{fu} = N_d N_t \langle \sigma v \rangle_{dt} \ Q_{dt} \tag{4.13}$$

to determine–for the case of $N_d = N_t = N_i/2$, $N_i = N_e$ and $T_i = T_e$ the magnetic pressure-limited fusion power density

$$P_{fu,mag} = \frac{\beta_{max}^2 B^4}{64\mu_o^2} \cdot \frac{\langle \sigma v \rangle_{dt}}{T_i^2} Q_{dt} \tag{4.14}$$

which is displayed in Fig. 4.3 as a function of the plasma temperature.

Another overriding consideration of plasma confinement relates to the ratio of total energy supplied to bring about fusion reactions and the total energy generated from fusion reactions. Commercial viability demands

$$E_{fu} >> E_{supply} \ . \tag{4.15}$$

Most toroidal confinement systems currently of interest are expected to operate

in a pulsed mode characterized by a burn time τ_b. Assuming the fusion power P_{fu} to be constant during τ_b, or to represent the average power over that interval, the fusion energy generated during this time is given by

$$E_{fu} = P_{fu} \cdot \tau_b = \langle \sigma v \rangle_{dt} N_d N_t Q_{dt} \tau_b \tag{4.16}$$

for d-t fusion. For perfect coupling of the energy supplied to an ensemble of deuterons, tritons, and electrons, we have

$$E_{supply} = \tfrac{3}{2} N_d kT_d + \tfrac{3}{2} N_t kT_t + \tfrac{3}{2} N_e kT_e \ . \tag{4.17}$$

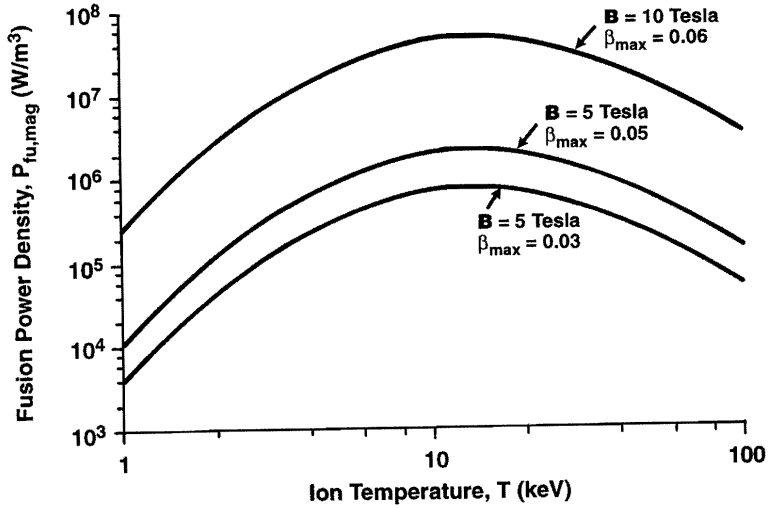

Fig. 4.3: Pressure-limited fusion power density in a magnetically confined d-t fusion plasma.

One may therefore identify an ideal energy breakeven of $E_{fu} = E_{supply}$ as defined by

$$\langle \sigma v \rangle_{dt} N_d N_t Q_{dt} \tau_b = \tfrac{3}{2} N_d kT_d + \tfrac{3}{2} N_t kT_t + \tfrac{3}{2} N_e kT_e \tag{4.18}$$

Imposing $N_d = N_t = N_i/2$, $N_i = N_e$, and $T_d = T_t = T_e = T$ we may simplify the relation to write for an ideal breakeven condition:

$$N_i \tau_b = \frac{12kT}{\langle \sigma v \rangle_{dt} Q_{dt}} \ . \tag{4.19}$$

Since Q_{dt} = 17.6 MeV and $\langle \sigma v \rangle_{dt}$ is known as a function of kT, we readily compute the product

$$N_i \tau_b \sim 10^{20} \ \text{s} \cdot \text{m}^{-3} \tag{4.20}$$

for kT ≈ 12 keV. Note that for fusion burn to be assured over the period τ_b, it is required that the actual magnetic confinement time, $\tau_{mc} > \tau_b$. The incorporation of other energy/power losses as well as energy conversion efficiencies suggests that this ideal breakeven is an absolute minimum, and operational pulsed fusion systems need to possess a product much higher. For instance, the accelerated motion of charged particles inevitably is accompanied by electro-magnetic radiation emission, as described by Eq.(3.39), which constitutes power loss from a confined plasma.

There exist various versions of Eq. (4.19)–depending upon what energy/power terms and conversion processes are included; collectively they are known as Lawson criteria in recognition of John Lawson who first published such analyses.

Problems

4.1 Verify the expression for the sonic speed in a compressed homogeneous deuterium-tritium ICF pellet, given in Eq. (4.4), by evaluating the defining equation $v_s^2 = dp/d\rho$ with ρ denoting the mass density of the medium in which the sonic wave is propagating. Assuming the sound propagation is rapid so that heat transfer does not occur, the adiabatic equation of state, $p\rho^{-\gamma} = C$, is applicable to the variations of pressure and density. Determine the constant C using the ideal gas law. To quantify γ, which represents the ratio of specific heats at fixed pressure and volume, respectively, c_p/c_V, use the relations $c_p - c_V = R$ (on a per mole basis) and $c_V = fR/2$ known from statistical thermodynamics, where R is the gas constant and f designates the number of degrees of freedom of motion (f = 3 for a monatomic gas, f = 5 for a diatomic gas, ...).

4.2 Compute v_s of Eq.(4.4) for typical hydrogen plasmas and compare to sound propagation in other media.

4.3 Re-examine the specification of a mean-time between fusions, Sec. 4.5, for the more general case of steady-state fusion reactions. How would you define, by analogy, the mean-free-path between fusions, λ_{fu}?

4.4 If 10% burnup of deuterium and tritium is achieved in a compressed sphere with R_b = 0.25 mm and fulfilling the burn condition of Eq. (4.8) with $N_{i,o}R_b = 5 \times 10^{-28}$ m^{-2}, at what rate would these pellets have to be injected into the reactor chamber of a 5.5 GW_t laser fusion power plant? The pellets contain deuterium and tritium in equal proportions. Power contributions from neutron-induced side reactions such as in lithium are to be ignored here.

4.5 Assess the minimum magnetic field strength required to confine a plasma having $N_i = N_e = 10^{20}$ m^{-3} and $T_i = 0.9\ T_e = 18$ keV, when $\beta_{max} = 8\%$.

4.6 Compute the maximum fusion power density of a magnetically confined d-h fusion plasma ($N_d = N_h$, $T_d = T_h = T_e$, no impurities) as limited by an assumed upper value of attainable field strength , B = 15 Tesla, dependent on the plasma temperature. Superimpose the result for $\beta_{max} = 2\%$ in Fig. 4.3.

5. Individual Charge Trajectories

The need for plasma confinement requires that some control on ion and electron motion be considered. While moving charges accordingly generate electromagnetic fields which additionally act on other moving particles, for the case of low densities, these induced fields–as well as the effect of collisions–may be neglected so that the trajectories of charged particles may be considered to be governed entirely by external field forces acting on them.

5.1 Equation of Motion

The basic relation which determines the motion of an individual charged particle of mass m and charge q in a combined electric and magnetic field is the equation

$$m\frac{d\mathbf{v}}{dt} = q\mathbf{E} + q(\mathbf{v}\times\mathbf{B}). \tag{5.1}$$

Here, **v** is the velocity vector of the particle at an arbitrary point in space and **E** and **B** are, respectively, the local electric field and magnetic flux density perceived by the particle; the magnetic flux density is commonly called the magnetic field. The last term in this equation is also known as the Lorentz force. We assume SI units so that the units of **E** are Newton/Coulomb while for **B** the units are Tesla; note that 1 Tesla (T) is defined as 1 Weber·m^{-2} (= 10^4 Gauss = 1 kg·s^{-2}·A^{-1}).

While gravitational forces are of importance in stellar fusion, they are negligible compared to the externally generated magnetic field forces and the established electric fields associated with fusion energy devices of common interest; hence, gravitational force effects need not be included for our purposes.

5.2 Homogeneous Electric Field

As an initial case, consider a domain in space for which **B** = **0** with only a constant electric field affecting the particle trajectory. Orienting the Cartesian coordinate system so that the z-axis points in the direction of **E**, Fig. 5.1, and imposing an arbitrary initial particle velocity at t = 0, referenced to the origin of the coordinate system, we simply write for Eq.(5.1)

$$m\frac{d\mathbf{v}}{dt} = q\,E_z\mathbf{k}\,, \tag{5.2}$$

where **k** is the unit vector in the z-direction. This vector representation for the motion of a single charged particle in an electric field can be decomposed into its constituent components

$$\frac{dv_x}{dt} = 0\,, \quad \frac{dv_y}{dt} = 0\,, \quad \frac{dv_z}{dt} = \left(\frac{q}{m}\right)E_z\,, \tag{5.3}$$

and these can be solved by inspection:

$$v_x = v_{x,o}\,, \quad v_y = v_{y,o}\,, \quad v_z = v_{z,o} + \left(\frac{q}{m}E_z\right)t\,. \tag{5.4}$$

Integrating again with respect to time gives the position of the charged particle at any time t:

$$x = v_{x,o}\,t\,, \quad y = v_{y,o}\,t\,, \quad z = v_{z,o}\,t + \tfrac{1}{2}\left(\frac{q}{m}E_z\right)t^2\,. \tag{5.5}$$

The corresponding trajectory for a positive ion is suggested in Fig. 5.2 with the particle located at the origin of the coordinate system at t = 0. This description therefore constitutes a parametric representation of a curve in Cartesian (x,y,z) space and corresponds to the trajectory of the charged particle under the action of an electric field only and for the initial condition specified.

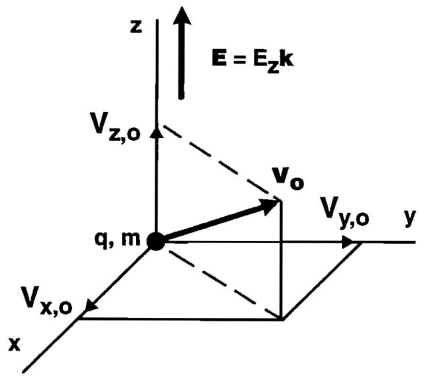

Fig. 5.1: Orientation of an electric field **E** acting on a particle of charge q and mass m.

The important feature to note is that the components of motion for this individual charged particle perpendicular to the **E**-field, that is v_x and v_y, do not change with time; however, the velocity component in the direction of the **E**-field, $v_z(t)$, is seen from Eq.(5.4) to linearly vary with time. The particle is accelerated in the direction of **E** for a positive charge and in the opposite

direction for a negative charge.

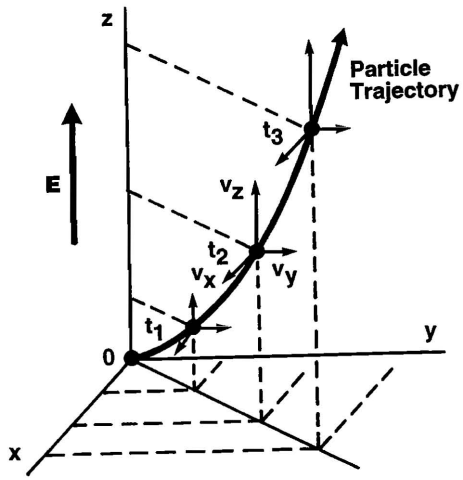

Fig. 5.2: Trajectory of a positively charged ion in a homogeneous electric field.

5.3 Homogeneous Magnetic Field

Consider now a single particle trajectory with **E** = **0** and **B** constant in the space of interest. The relevant governing equation now becomes

$$m\frac{d\mathbf{v}}{dt} = q(\mathbf{v}\times\mathbf{B}) \tag{5.6}$$

and by the definition of a vector cross product, the force on the particle is here perpendicular to both **v** and **B**. Writing Eq.(5.6) in terms of its vector components, we find

$$\frac{d}{dt}\left(v_x\mathbf{i} + v_y\mathbf{j} + v_z\mathbf{k}\right) = \frac{q}{m}\left[\left(v_x\mathbf{i} + v_y\mathbf{j} + v_z\mathbf{k}\right)\times\left(B_x\mathbf{i} + B_y\mathbf{j} + B_z\mathbf{k}\right)\right] \tag{5.7}$$

where **i**, **j** and **k** are orthogonal unit vectors along the x, y and z axes, respectively.

Orienting this coordinate system so that the z-axis is parallel to the **B**-field, thereby imposing $B_x = B_y = 0$, Fig. 5.3, and equating the appropriate vector components of Eq.(5.7), we obtain the following set of differential equations together with their initial conditions:

$$\frac{dv_x}{dt} = \left(\frac{q\,B_z}{m}\right) v_y\,, \quad v_x(0) = v_{x,o}\,, \tag{5.8a}$$

$$\frac{dv_y}{dt} = -\left(\frac{q\,B_z}{m}\right) v_x\,, \quad v_y(0) = v_{y,o} \tag{5.8b}$$

and

$$\frac{dv_z}{dt} = 0\,. \quad v_z(0) = v_{z,o}\,. \tag{5.8c}$$

The interesting feature here is that $v_x(t)$ and $v_y(t)$ are mutually coupled but that $v_z(t)$ is independent of the former. Hence, the z-component is therefore straightforward and based on Eq.(5.8c), we have

$$v_z(t) = v_{z,o} = v_{\|} \tag{5.9}$$

which is a constant with the parallel line subscripts referring to the direction of the **B**-field. Then with the reference z-coordinate as $z(0) = z_o$, another integration gives

$$z(t) = z_o + v_{\|}t \tag{5.10}$$

with the trajectory of the charged particle motion in the z-direction thus established.

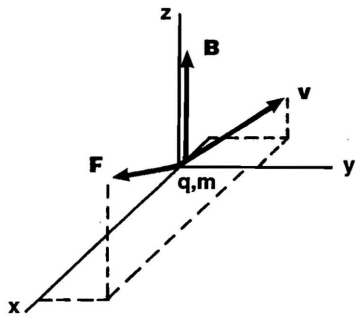

Fig. 5.3: Orientation of a magnetic field so that **B** is normal to the x-y plane and **F** is perpendicular to both **B** and **v**.

To solve for the velocity and position components perpendicular to the **B**-field direction–that is $v_x(t)$, $v_y(t)$, x(t) and y(t)–we first uncouple Eqs.(5.8a) and (5.8b) by differentiation and substitution to obtain

$$\frac{d^2 v_x}{dt^2} = \left(\frac{q\,B_z}{m}\right)\frac{dv_y}{dt} = -\omega_g^2 v_x \tag{5.11a}$$

and

$$\frac{d^2 v_y}{dt^2} = -\left(\frac{q\,B_z}{m}\right)\frac{dv_x}{dt} = -\omega_g^2 v_y\,, \tag{5.11b}$$

where, upon recognizing that both Eq.(5.11a) and Eq.(5.11b) describe a harmonic oscillation with the same frequency which results in a circular motion of the particle given suitable initial conditions, we have introduced the gyration frequency–sometimes also called the gyrofrequency or cyclotron frequency–as

$$\omega_g = \frac{|q|\,B_z}{m}\,. \tag{5.12}$$

Evidently, the following forms satisfy Eq.(5.11):

$$v_x(t) = A_x \cos(\omega_g t) + D_x \sin(\omega_g t)\,, \tag{5.13a}$$

$$v_y(t) = A_y \cos(\omega_g t) + D_y \sin(\omega_g t) \tag{5.13b}$$

with A_x, A_y, D_x and D_y constants to be determined for the case of interest.

It is known that a plasma possesses diamagnetic properties. This means that the direction of the magnetic field generated by the moving charged particles is opposite to that of the externally imposed field. Therefore, not only must the equations resulting from Eq.(5.6) be satisfied but the moving charged particle representing in fact a current flow along its trajectory must generate a magnetic field in opposition to **B**. Some thought and analytical experimentation with Eqs.(5.13) yields velocity components for a positive ion as

$$v_x(t) = v_o \cos(\omega_g t + \phi) \tag{5.14a}$$

and

$$v_y(t) = -v_o \sin(\omega_g t + \phi) \tag{5.14b}$$

where v_o is a positive constant speed and ϕ is the initial phase angle. For a negatively charged particle, Eq.(5.14b) will change its sign, while Eq.(5.14a) remains unchanged. Then, with $v_x(t)$ and $v_y(t)$ thus determined, a further integration yields x(t) and y(t) as

$$x(t) = x_o + \frac{v_o}{\omega_g}\sin(\omega_g t + \phi) \tag{5.15a}$$

$$y(t) = y_o + sign(q)\frac{v_o}{\omega_g}\cos(\omega_g t + \phi) \tag{5.15b}$$

describing thereby a circular orbit about the reference coordinate (x_o, y_o) for an arbitrary charge of magnitude q and sign designated by sign(q). This coordinate constitutes a so-called "guiding" centre which can, in view of Eq.(5.9), move at a constant speed in the z-direction. The gyration in 3-dimensions would therefore appear as a helix of constant pitch.

From Eqs.(5.14) it follows that the particle speed in the plane perpendicular to the magnetic field is a conserved quantity, and hence we write

$$v_o = \sqrt{v_x^2 + v_y^2} = v_{\perp}\,, \tag{5.16}$$

in order to denote the velocity component perpendicular to **B**. Evidently, if $v_{\|} = 0$,

the particle trajectory is purely circular, and the corresponding radius is obviously determined by

$$r_g = \frac{v_\perp}{\omega_g} = \frac{v_\perp m}{|q| B_z} . \tag{5.17}$$

The label gyroradius–as a companion expression to the gyrofrequency ω_g–is generally assigned to this term r_g although the name Larmor radius is also often used.

From the above it is evident that a heavy ion will have a larger radius than a lighter ion at the same $v_\perp$, and, by definition of ω_g, Eq.(5.12), an electron will possess a much higher angular frequency than a proton. Figure 5.4 depicts the circular trajectory of an ion and an electron as a projection of motion on to the x-y plane under the action of a uniform magnetic field $\mathbf{B} = B_z\mathbf{k}$. A useful rule to remember is that with **B** pointing into the plane of the page, an ion circles counterclockwise while electrons circle clockwise. Note that this is consistent with the diamagnetic property of a plasma by noting that, at the (x_o,y_o) coordinate, the self-generated **B**-field points in the opposite direction to the external magnetic field vector **B**.

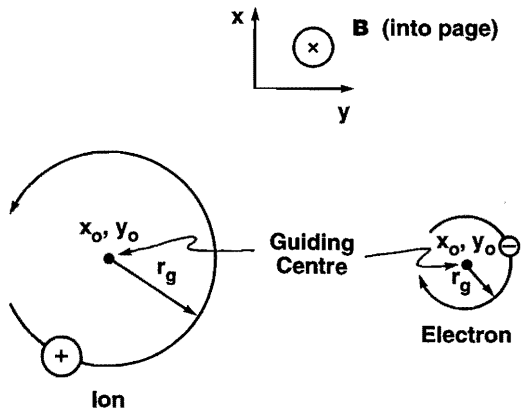

Fig. 5.4: Projection of ion and electron motion on the x-y plane which is perpendicular to the direction of the magnetic field vector.

With a constant velocity component parallel to the **B**-field and a time-invariant circular projection in the perpendicular plane, the particle trajectory in 3-dimensions represents a helical pattern along the **B**-line as suggested in Fig.5.5; note that $v_{z,o} = v_\parallel$ solely determines the axial motion. The pitch of the helix is also suggested in Fig.5.5 and is given by

$$\Delta z = z\left(t + \frac{2\pi r_g}{v_\perp}\right) - z(t) . \tag{5.18}$$

Using Eq.(5.10) gives

$$\begin{aligned} \Delta z &= \left[z_o + v_\parallel\left(t + \frac{2\pi r_g}{v_\perp}\right)\right] - \left[z_o + v_\parallel t\right] \\ &= 2\pi\left(\frac{v_\parallel}{v_\perp}\right) r_g \\ &= 2\pi\frac{v_\parallel}{\omega_g} \end{aligned} \tag{5.19}$$

which is constant for our case. Thus, an isolated charged particle in a constant, homogeneous magnetic field traces out a helical trajectory of constant radius, frequency and pitch.

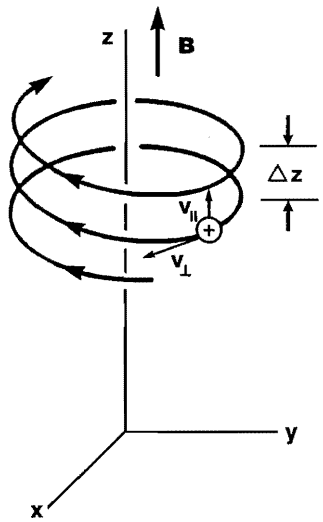

Fig. 5.5: Trajectory of an isolated ion in a uniform magnetic field.

5.4 Combined Electric and Magnetic Field

Consider next the effect of a combined **E** and **B** field on the trajectory of a charged particle. With both fields uniform and constant throughout our space of

interest, the trajectory is expected to be more complex since it will combine features of the two trajectories of Figs. 5.2 and 5.5.

With the **B**-field and **E**-field possessing arbitrary directions, it is useful to orient the Cartesian coordinate systems so that the z-axis is parallel to **B** with **E** in the x-z plane, Fig. 5.6. The equation of motion, Eq.(5.1), is now expanded to give

$$m\frac{d}{dt}\left(v_x\mathbf{i}+v_y\mathbf{j}+v_z\mathbf{k}\right)=q\left[\left(E_x\mathbf{i}+E_z\mathbf{k}\right)+\left(v_x\mathbf{i}+v_y\mathbf{j}+v_z\mathbf{k}\right)\times\left(B_z\mathbf{k}\right)\right] \quad (5.20)$$

so that the velocity components must satisfy

$$\frac{dv_x}{dt}=\frac{q}{m}E_x+\frac{q}{m}B_z v_y=\frac{q}{m}E_x+\omega_g v_y\, sign(q)\,, \quad (5.21a)$$

$$\frac{dv}{dt}=-\frac{q}{m}B_z v_x=-\omega_g v_x\, sign(q), \quad (5.21b)$$

and

$$\frac{dv_z}{dt}=\frac{q}{m}E_z\,. \quad (5.21c)$$

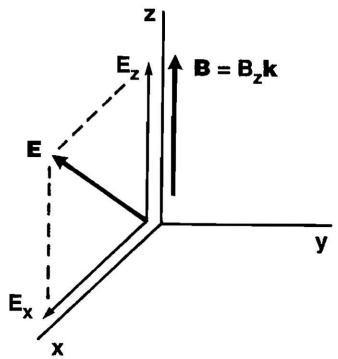

Fig. 5.6: Orientation of a magnetic field **B** and electric field **E**.

Here, the gyrofrequency ω_g, Eq.(5.12), has again appeared and the charge sign of the particle is indicated by sign (q), thereby specifying the direction of gyration. The velocity components v_x and v_y may be uncoupled by differentiation and substitution of Eqs.(5.21a) and (5.21b):

$$\frac{d^2 v_x}{dt^2}=0+\omega_g\frac{dv_y}{dt}sign(q)=-\omega_g^2 v_x \quad (5.22a)$$

and

$$\frac{d^2 v_y}{dt^2}=-\omega_g\frac{dv_x}{dt}sign(q)$$

$$=-\omega_g\, sign(q)\left(\frac{q}{m}E_x+\omega_g v_y\, sign(q)\right) \quad (5.22b)$$

$$=-\omega_g^2\left(\frac{E_x}{B_z}+v_y\right).$$

With E_x, B_z, and ω_g as constants, this last expression may therefore be written as

$$\frac{d^2 v_y^*}{dt^2}=-\omega_g^2 v_y^* \quad (5.23)$$

where

$$v_y^*=\frac{E_x}{B_z}+v_y\,. \quad (5.24)$$

The useful result here is that with this definition of v_y^*, the problem of determining the particle trajectory in a combined **E** and **B**-field, Eqs.(5.22a) and (5.23), has been cast into the mathematical framework of a **B**-field acting alone as in the preceding section. Using Eqs.(5.14) and (5.16), we find that

$$v_x=v_o^*\cos(\omega_g t+\phi^*) \quad (5.25a)$$

and

$$v_y^*=-v_o^*\sin(\omega_g t+\phi^*)sign(q) \quad (5.25b)$$

where the speed is now

$$v_o^*=\sqrt{v_{x,o}^2+(v_{y,o}+E_x/B_z)^2} \quad (5.26)$$

and ϕ^* relates to the previous initial phase angle by

$$v_o^*\cos\phi^*=\sqrt{v_{x,o}^2+v_{y,o}^2}\cos\phi\,. \quad (5.27)$$

Substituting for v_y^* in Eq. (5.24) and further introducing the solution for v_z, as evident from Eq.(5.21c), yields the following set of velocity components:

$$v_x=v_o^*\cos(\omega_g t+\phi^*)\,, \quad (5.28a)$$

$$v_y=-v_o^*\sin(\omega_g t+\phi^*)sign(q)-\frac{E_x}{B_z} \quad (5.28b)$$

and

$$v_z=v_{\|}+\left(\frac{q\,E_z}{m}\right)t\,. \quad (5.28c)$$

The associated (x,y,z) coordinates follow from a further integration to yield

$$x=x_o+\frac{v_o^*}{\omega_g}\sin(\omega_g t+\phi^*)\,, \quad (5.29a)$$

$$y = y_o + \frac{v_o^*}{\omega_g}\cos(\omega_g t + \phi^*)sign(q) - \frac{E_x}{B_z}t \qquad (5.29b)$$

and

$$z = z_o + v_{\|}t + \tfrac{1}{2}\left(\frac{q E_z}{m}\right)t^2 . \qquad (5.29c)$$

These equations, Eqs.(5.28) and (5.29), show that the charged particle still retains its cyclic motion but that it drifts in the negative y-direction for $E_x > 0$, Fig. 5.7, and oppositely if $E_x < 0$. Hence, the guiding centre's drift is in the direction perpendicular to both the **B**-field and **E**-field and in contrast to the preceding ($\mathbf{E} = \mathbf{0}$, $\mathbf{B} \neq \mathbf{0}$) case, ion and electron motion across the field lines now occur. Additionally, the pitch increases with time–Eqs.(5.28c) and (5.29c)–so that the trajectory resembles a slanted helix with increasing pitch.

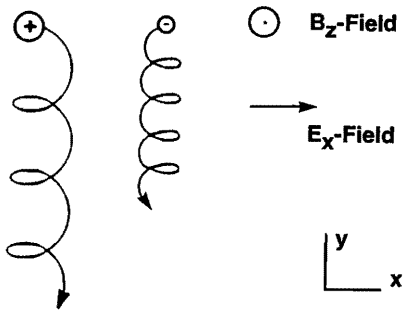

Fig. 5.7: Positive ion and electron drift in a combined uniform magnetic and electric field.

We now consider a generalization of the drift velocity caused by an arbitrary force **F** on a charged particle moving in an uniform **B**-field. To begin, we decompose the particle velocity into the components

$$\mathbf{v} = \mathbf{v}_{gc} + \mathbf{v}_g \qquad (5.30)$$

where $\mathbf{v}_{gc}$ is the velocity of guiding centre motion and $\mathbf{v}_g$ is the velocity of gyration relative to the guiding centre. The equation of motion is now written as

$$m\frac{d\,\mathbf{v}_{gc}}{dt} + m\frac{d\,\mathbf{v}_g}{dt} = \mathbf{F} + q(\mathbf{v}_{gc}\times\mathbf{B}) + q(\mathbf{v}_g\times\mathbf{B}) . \qquad (5.31)$$

Evidently the terms describing the circular motion, i.e. the second term on the left and the third on the right cancel one another according to Eq.(5.6). Further, in a static field exhibiting straight **B**-field lines the charged particle motion will be such that, averaged over one gyroperiod τ, the total acceleration perpendicular to **B** must vanish; that is, the guiding centre is not accelerated in any direction perpendicular to **B**. Therefore, we average the transverse part of Eq.(5.31) over

this gyroperiod $\tau = 2\pi/\omega_g$ to write

$$0 = \frac{1}{\tau}\int_0^\tau \left(m\frac{d\,\mathbf{v}_{gc}}{dt}\right)_\perp dt = \frac{1}{\tau}\int_0^\tau (\mathbf{F}_\perp + q(\mathbf{v}_{gc}\times\mathbf{B}))dt . \qquad (5.32)$$

This now specifies

$$\bar{\mathbf{F}}_\perp = -q(\bar{\mathbf{v}}_{gc}\times\mathbf{B}) \qquad (5.33)$$

with $\bar{\mathbf{F}}_\perp$ representing the gyro-period averaged force acting perpendicular to **B** and $\bar{\mathbf{v}}_{gc}$ the average velocity of the guiding centre, respectively. Taking next the cross-products with **B**, we obtain

$$\bar{\mathbf{F}}\times\mathbf{B} = \bar{\mathbf{F}}_\perp\times\mathbf{B} = q\left[\bar{\mathbf{v}}_{gc}B^2 - \mathbf{B}(\bar{\mathbf{v}}_{gc}\cdot\mathbf{B})\right] \qquad (5.34)$$

where a vector product identity has been utilized for the last step. Note from Eq.(5.31) that the motion of the guiding centre parallel to the magnetic field **B** can only be affected by the parallel component of **F**. Then, since $\mathbf{v}_g$ is perpendicular to **B**, the velocity component $v_{gc,\|} = v_{\|}$ and is readily seen to be given by

$$v_{gc,\|}(t) = v_{gc,\|}(0) + \frac{1}{m}\int F_{\|}\,dt . \qquad (5.35)$$

Of greater interest here is the perpendicular component $v_{gc,\perp}$ which is found from Eq.(5.34) as

$$\bar{\mathbf{v}}_{gc,\perp} = \frac{\bar{\mathbf{F}}\times\mathbf{B}}{qB^2} \qquad (5.36)$$

because $(\bar{\mathbf{v}}_{gc,\perp}\cdot\mathbf{B}) = \mathbf{0}$. This identifies what is called the drift velocity due to the force **F**, i.e.

$$\bar{\mathbf{v}}_{gc,\perp} = \mathbf{v}_{DF} . \qquad (5.37)$$

This generalization allows us to specify an expression if the additional force acting in a static magnetic field domain is an electric force $\mathbf{F} = q\mathbf{E}$, so that the drift velocity due to a stationary electric field is

$$\mathbf{v}_{D,E} = \frac{\mathbf{E}\times\mathbf{B}}{B^2} . \qquad (5.38)$$

The label "**E** × **B** drift" is frequently used in this context. Note that the drift is evidently independent of the mass and charge of the particle of interest, and consistent with the drift velocity term in Eq.(5.28b), i.e. $(-E_x / B_z)$.

5.5 Spatially Varying Magnetic Field

Each of the preceding cases involved a **B**-field taken to be uniform throughout the space of interest. Such an idealization is, in practice, impossible although it

can be approached to some degree by using sufficiently large magnet or coil arrangements. In general, however, it often becomes necessary to incorporate a space dependent **B**-field which governs the particles' motion. The associated equation of motion is hence written as

$$m\frac{d\mathbf{v}}{dt} = q\left[\mathbf{v}\times\mathbf{B}(\mathbf{r})\right]. \tag{5.39}$$

A comprehensive analysis of this equation for a most general case may obscure some important instructional aspects so that a more intuitive approach has merit; this approach also provides for a convenient association with the preceding analysis while still leading to some useful generalizations.

We consider therefore a dominant magnetic field in the z-direction characterized by an increasing strength in the y-direction; that is, a constant non-zero gradient of the magnetic field strength, ∇B, exists everywhere given by

$$\nabla B = \frac{\partial B_z}{\partial y}\,\mathbf{j}. \tag{5.40}$$

Figure 5.8 provides a graphical depiction of this **B**-field showing also a test ion with specified initial velocity components.

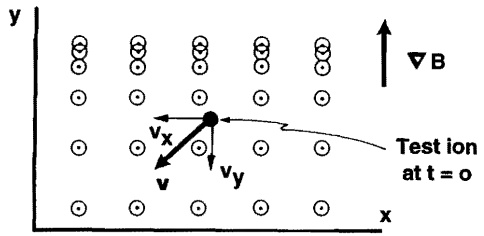

Fig. 5.8: Illustration of a spatially varying magnetic field **B** with the field lines pointing vertically up from the page.

From the previous analysis of the motion of a charged particle in a uniform **B**-field, it is known that the radius of gyration in the plane perpendicular to the local **B**-field is given by

$$r_g = \frac{v_\perp}{\omega_g} = \frac{v_\perp m}{|q|B} \tag{5.41}$$

where B is the local magnetic field magnitude at the point where the charged particle's guiding centre is located; thus, the gyroradius r_g varies inversely with B. Any motion in the z-direction will be additive and depends upon the initial $v_\parallel$ component; for reasons of algebraic simplification and pictorial clarity, we may therefore take $v_\parallel = 0$.

Referring to Eq.(5.41) and Fig. 5.8, it is evident therefore that an isolated

charged test particle will trace out a trajectory whose radius of curvature becomes larger in the weaker magnetic field and smaller where the **B**-field is stronger. We can translate this effect into a process which tends to transform a circular path into a shifting cycloid-like path with the consequence that the particle trajectory now tends to cross magnetic field lines as suggested in Fig. 5.9.

Note that the radius of gyration, Eq.(5.41), is directly proportional to the mass of the particle and that the sign of the charge enters into the direction of the trajectory. This is also indicated in Fig. 5.9 for a positively and negatively charged particle, although not to scale. The feature that the gradient causes a drift of the positive ions in one direction and for electrons in the opposite direction has important consequences because the resulting charge separation introduces an electric field which, in a plasma, can contribute to plasma oscillations and instability, which we will further discuss in subsequent chapters.

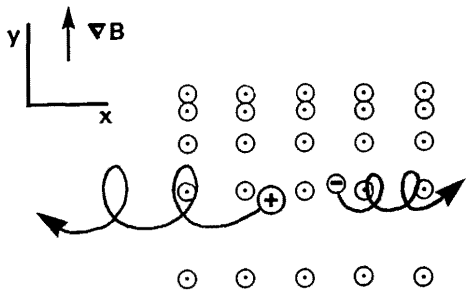

Fig. 5.9: Motion of a positively and negatively charged particle in a spatially varying magnetic field.

With an intuitive approach of the gradient-B drift phenomenon thus suggested, we consider next an approximate though useful analytical representation. The first approximation to be introduced is that for the case of a weak magnetic field inhomogeneity over distances corresponding to a gyroradius, that is, $|\nabla B|/B << 1/r_g$, only the first two terms of a Taylor expansion of $B_z(y)$ are retained, i.e.

$$B_z(y) \approx B_z(y_o) + (y - y_o)\left.\frac{dB_z}{dy}\right|_{y=y_o} \tag{5.42}$$

where y_o corresponds to the y-coordinate of the guiding centre. Extending to the vector form for Eq.(5.42), we write

$$\mathbf{B}(y) \approx \mathbf{B}_o + (y - y_o)|\nabla B|\frac{\mathbf{B}_o}{B_o} \tag{5.43}$$

where now $\mathbf{B}_o = \mathbf{B}(y_o)$. We next expand the equation of motion, Eq.(5.39), and write

$$m\frac{d\mathbf{v}}{dt} = q(\mathbf{v}\times\mathbf{B}_o)\left[1 + (y - y_o)\frac{|\nabla B|}{B_o}\right]. \tag{5.44}$$

Recalling our preceding discussion of a drift caused by a general force **F** applied to a charged particle in a uniform **B**-field, we decompose **v** as in Eqs.(5.30) and (5.31) to write

$$m\frac{d\,\mathbf{v}_{gc}}{dt} = q(\mathbf{v}_{gc}\times\mathbf{B}_o) + q\frac{|\nabla B|}{B_o}(y - y_o)[(\mathbf{v}_{gc} + \mathbf{v}_g)\times\mathbf{B}_o] \tag{5.45}$$

with the terms describing gyromotion in a uniform field $\mathbf{B}_o$ having been canceled. Comparison of Eq.(5.45) with Eq.(5.31) makes it evident that the last term in Eq.(5.45) can be identified as the force term **F** responsible for the ∇B drift. Following our analysis involving Eqs.(5.32) to (5.36), we need **F**–which points in a direction perpendicular to $\mathbf{B}_o$–to be averaged over a gyroperiod τ so that

$$\overline{\mathbf{F}} = q\frac{|\nabla B|}{B_o}\cdot\frac{1}{\tau}\int_0^{\tau}[y(t) - y_o]\,[\mathbf{v}(t)\times\mathbf{B}_o]dt\,. \tag{5.46}$$

Further, as a first order approximation of the product $|\nabla B|(y(t) - y_o)\mathbf{v}(t)$ in the above expression, we use for y(t) and **v**(t) the (undisturbed) uniform **B**-field solution of Eqs.(5.9), (5.14) and (5.15b) to write

$$y(t) - y_o \approx sign(q)\frac{v_\perp}{\omega_g}\cos(\omega_g t + \phi) \tag{5.47}$$

and

$$\mathbf{v}(t) \approx \begin{pmatrix} v_\perp\cos(\omega_g t + \phi) \\ -sign(q)v_\perp\sin(\omega_g t + \phi) \\ v_\parallel \end{pmatrix}. \tag{5.48}$$

Upon substitution of this expression into Eq.(5.46) and performing the vector cross product–recalling also that $\mathbf{B}_o$ points into the positive z-direction–we obtain

$$\begin{aligned}\overline{\mathbf{F}} &= q\frac{|\nabla B|}{B_o}\frac{1}{\tau}\int_0^{\tau}\frac{v_\perp^2}{\omega_g}B_o\cos(\omega_g t + \phi)\begin{pmatrix} -\sin(\omega_g t + \phi) \\ -sign(q)\cos(\omega_g t + \phi) \\ 0 \end{pmatrix}dt \\ &= q\frac{|\nabla B|}{B_o}\left[-sign(q)\frac{\omega_g}{2\pi}\int_0^{2\pi/\omega_g}\frac{v_\perp^2}{\omega_g}B_o\cos^2(\omega_g t + \phi)dt\right]\mathbf{j}\end{aligned} \tag{5.49}$$

where $\tau = 2\pi/\omega_g$ has been substituted and **j** is the unit vector in the y-direction;

note that integration of the product sin( )cos( ) provides no contribution by reason of orthogonality. Hence, integration of Eq. (5.49) leads to

$$\overline{\mathbf{F}} \approx -|q|\left(\frac{dB}{dy}\right)\left(\frac{v_\perp^2}{2\omega_g}\right)\mathbf{j} = -|q|\frac{v_\perp^2}{2\omega_g}\nabla B\,. \tag{5.50}$$

This latter expression is a general formulation since the y-axis was arbitrarily chosen due to the geometry of Sec. 5.3.

Finally, recalling Eqs.(5.36) and (5.37), we find the grad-B drift velocity as

$$\mathbf{v}_{D,\nabla B} = sign(q)\frac{v_\perp^2}{2\omega_g}\frac{\mathbf{B}\times\nabla B}{B^2} \tag{5.51}$$

and thus the positive ions and negative electrons drift across B-field lines in opposite directions in a non-uniform magnetic field as displayed in Fig. 5.9.

In subsequent chapters, we will discover that fusion devices which utilize magnetic fields for confinement of the reacting ions involve very complex magnetic field topologies. Not only are there electric fields and spatially varying magnetic fields present–thus giving rise to the drift velocities $\mathbf{v}_{D,E}$ and $\mathbf{v}_{D,\nabla B}$ just discussed–but there are additional complexities due to curvature in the magnetic field lines and gradients along these field lines. We thus now formulate expressions for the effective forces and resulting drift velocities due to these inhomogeneities in the **B**-fields, analogous to Eqs.(5.38) and (5.51).

5.6 Curvature Drift

Consider then charged particle motion in a magnetic field **B** whose field lines possess a radius of curvature R. In examining such a case we specify here the curved magnetic field lines by

$$\mathbf{B} = B_o\mathbf{k} + B_o\frac{z}{R}\mathbf{j} \tag{5.52}$$

when referred to in the vicinity of the y-axis, that is for $|z/R| << 1$. A graphical depiction is provided in Fig. 5.10.

Introducing this field configuration, Eq. (5.52), into the Lorentz-force equation, Eq.(5.6), yields

$$m\frac{d\mathbf{v}}{dt} = q(\mathbf{v}\times B_o\mathbf{k}) + q\left(\mathbf{v}\times\frac{z}{R}B_o\mathbf{j}\right) \tag{5.53}$$

which–upon decomposition according to Eq. (5.30) and subsequent cancellation of the gyration terms–reads as

$$m\frac{d\,\mathbf{v}_{gc}}{dt} = q\,B_o(\mathbf{v}_{gc}\times\mathbf{k}) + q\,B_o\frac{z}{R}(\mathbf{v}\times\mathbf{j})\,. \tag{5.54}$$

For small curvatures, i.e. $|z/R| << 1$, we may, as in the previous cases, approximate the product $z(\mathbf{v}\times\mathbf{j})$ by the undisturbed uniform solutions given in

Eqs.(5.10) and (5.48), respectively, and thus obtain

$$\frac{d\,\mathbf{v}_{gc}}{dt} = \frac{q\,B_o}{m}\left(\mathbf{v}_{gc}\times\mathbf{k}\right) + \frac{q\,B_o\,v_{\parallel}\,t}{mR}\left[-\,v_{\parallel}\mathbf{i} + v_{\perp}\cos(\omega_g t)\mathbf{k}\right] \tag{5.55}$$

where we specified $z_o = 0$ and the initial phase angle of Eq. (5.48) as $\phi = 0$. Further substituting qB_o/m by Eq. (5.12), we separate Eq. (5.55) into its Cartesian components and write

$$\frac{dv_{gc,x}}{dt} = sign(q)\;\omega_g\left(v_{gc,y} - \frac{v_{\parallel}^2}{R}t\right) \tag{5.56a}$$

$$\frac{dv_{gc,y}}{dt} = -sign(q)\,\omega_g\,v_{gc,x} \tag{5.56b}$$

$$\frac{dv_{gc,z}}{dt} = sign(q)\,\omega_g\,\frac{v_{\parallel}\,v_{\perp}}{R}\,t\cos(\omega_g t)\,. \tag{5.56c}$$

Apparently, Eq. (5.56c) can be solved straightforwardly upon knowing that $v_{gc,z}(0) = v_{\parallel}$. Averaging the resulting velocity $v_{gc,z}$ over a gyration period will suppress the small oscillations with the cyclotron frequency ω_g and indicate a steady drift anti-parallel to the **B**-field; this velocity drift, however, is seen to depend on the initial condition, $v_{\perp} = v_o$, and is therefore not classified as a drift.

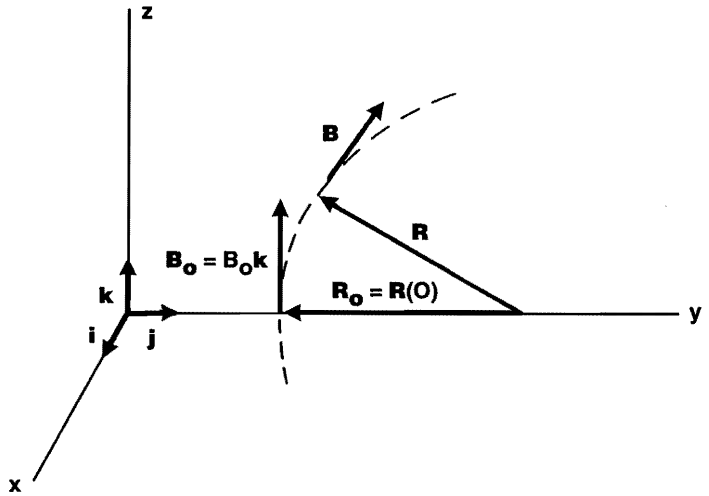

Fig. 5.10: Topology of the curved magnetic field $\mathbf{B} = B_o\mathbf{k} + B_o(z/R)\mathbf{j}$ with **R** representing the radius of curvature vector.

To solve for the velocity components perpendicular to **B** we uncouple the

mutual dependencies of Eqs. (5.56a) and (5.56b) by differentiation and subsequent substitution to obtain

$$\frac{d^2 v_{gc,x}}{dt^2} + \omega_g^2\,v_{gc,x} = -sign(q)\,\omega_g\,\frac{v_{\parallel}^2}{R}\,. \tag{5.57}$$

The solution of this inhomogeneous differential equation is accomplished by summing of the homogeneous solution of the form $A\cos(\omega_g t + \alpha)$ and a stationary solution to the inhomogeneous equation, which, by inspection of Eq.(5.57), we take as $(\text{sign}(q)v_{\perp}^2/\omega_g R)$. Referring to the initial conditions $v_{gc,x}(0)=v_{gc,y}(0)=0$ associated with the undisturbed field at $z(0) = 0$, we determine the constants A and α and finally find

$$v_{gc,x} = sign(q)\frac{v_{\parallel}^2}{\omega_g R}\left[\cos(\omega_g t) - 1\right] \tag{5.58a}$$

and

$$v_{gc,y} = \frac{v_{\parallel}^2}{\omega_g R}\left[\omega_g t - \sin(\omega_g t)\right]\,. \tag{5.58b}$$

The resulting drifts are, as preceedingly, revealed by averaging over a gyration period and are thus

$$\overline{\mathbf{v}_{gc,x}} = -sign(q)\frac{v_{\parallel}^2}{\omega_g R}\,\mathbf{i} \tag{5.59a}$$

and

$$\overline{\mathbf{v}_{gc,y}} = \frac{v_{\parallel}^2}{R}\bar{t}\,\mathbf{j} = \mathbf{a}_{cp}\bar{t} \tag{5.59b}$$

where $\bar{t}$ represents an average length of time corresponding to one half of the interval of averaging. The latter equation clearly demonstrates that the guiding centre is accelerated in the direction of **j** at the magnitude $v_{\parallel}^2/R$ which, of course, is known to be the centripetal acceleration $\mathbf{a}_{cp}$ required to make the particle follow the curved **B**-field line. The only real *steady* drift is then accounted for by (Eq. 5.59a), in which we substitute according to the geometry of Fig. 5.10

$$\mathbf{i} = \mathbf{j}\times\mathbf{k} = -\frac{\mathbf{R}_o}{R}\times\frac{\mathbf{B}_o}{B_o} \tag{5.60}$$

and reintroduce $\omega_g = |q|B_o/m$ to derive the curvature drift velocity as

$$\mathbf{v}_{D,R} = \overline{\mathbf{v}_{gc,x}} = \frac{mv_{\parallel}^2}{q\,B_o^2}\frac{\mathbf{R}_o\times\mathbf{B}_o}{R^2} \tag{5.61}$$

which is thus again dependent upon the sign of the charge. Fig. 5.11 illustrates this drift of an ion spiraling around a curved magnetic field line.

A curved **B**-field is shown below to be accompanied by a gradient **B**-field, thus both specific drift velocity's components add to yield the resultant drift. We remark that, although the expressions for the different drift velocities derived

here are correct, the assumptions and approximations used in the derivation are inconsistent in the sense that the suggested nonuniform **B**-fields do not satisfy Maxwell's equations

$$\nabla \times \mathbf{B} = \mathbf{0} \tag{5.62}$$

and

$$\nabla \cdot \mathbf{B} = 0 . \tag{5.63}$$

In order that these fundamental equations are met, it is seen that an inhomogeneous magnetic field has always to be associated with some curvature and vice versa. Hence grad-B drift and curvature drift will occur simultaneously.

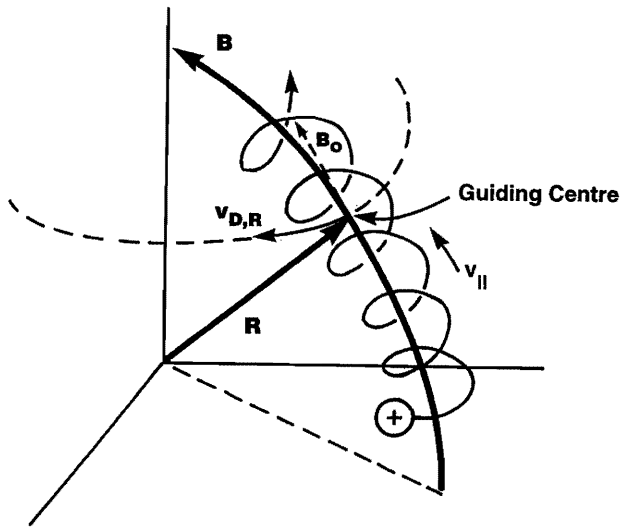

Fig. 5.11: Illustration of curvature drift of a positive ion moving along a curved **B**-field line.

5.7 Axial Field Variations

A magnetic field which varies spatially in strength in the direction of the field is of considerable importance in various mirror configurations–Fig. 4.2b. We suggest such a general case in Fig.5.12 and assess its effect on ion motion.

Cylindrical coordinates, (r,θ,z) in Fig. 5.12, will serve us well for which Maxwell's Second Equation, Eq.(5.63), gives

$$\nabla \cdot \mathbf{B} = \frac{1}{r}\frac{\partial}{\partial r}(r B_r) + \frac{1}{r}\frac{\partial B_\theta}{\partial \theta} + \frac{\partial B_z}{\partial z} = 0 . \tag{5.64}$$

Axial symmetry is generally expected to hold so that $\partial B_\theta/\partial\theta = 0$ and we obtain

$$B_r = -\frac{1}{r}\int_0^r r' \frac{\partial B_z}{\partial z} dr' \approx -\frac{r}{2}\frac{\partial B_z}{\partial z} \tag{5.65}$$

with the boundary condition B_r (r = 0) = 0 and $\partial B_z/\partial z$ taken to be independent of r. Then, assuming $B_\theta = 0$, we write

$$\mathbf{B} = B_r \mathbf{e}_r + B_z \mathbf{e}_z \tag{5.66}$$

where $\mathbf{e}_r$ and $\mathbf{e}_z$ are the radial and axial unit vectors in cylindrical geometry, respectively, Fig. 5.12. The corresponding equation of motion of a charged particle in this field is

$$m\frac{d\mathbf{v}}{dt} = q(\mathbf{v} \times B_z \mathbf{e}_z) + q(\mathbf{v} \times B_r \mathbf{e}_r) . \tag{5.67}$$

The first term is recognized as the force responsible for particle gyration about B_z and also as that which leads to a grad-B drift, e.g. Eq.(5.51), when the dependence of B_z on r becomes significant. The second term, explicitly written as

$$q(\mathbf{v} \times B_r \mathbf{e}_r) = -q\, v_\theta B_r \mathbf{e}_z + q\, v_z B_r \mathbf{e}_\theta \tag{5.68}$$

contains a force parallel or antiparallel to the field on the axis and an azimuthal force. While the latter urges the particles to drift in the radial direction thus rendering their guiding centres to follow the specific magnetic field lines, the parallel force component will accelerate or, respectively, decelerate ions and electrons along the z-axis depending on the direction of their motion. With the aid of Eq. (5.65) this force component can be expressed as

$$F_{||} = \tfrac{1}{2} q\, v_\theta r \frac{\partial B_z}{\partial z} . \tag{5.69}$$

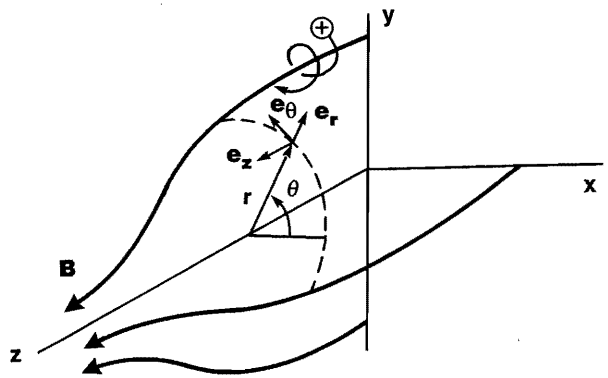

Fig. 5.12: Ion motion in a convergent magnetic field represented in cylindrical geometry.

We may now recognize the associated effect on the guiding centre by taking again an average $F_\parallel$ over a gyroperiod. Specifically taking the particles to gyrate around the central **B**-line at r = 0 renders the relation

$$v_\theta = -sign(q)v_\perp \tag{5.70}$$

so that for $r = r_g$, we obtain

$$F_\parallel = -\tfrac{1}{2}|q|v_\perp r_g \frac{\partial B_z}{\partial z} . \tag{5.71}$$

Upon substitution of r_g by Eq. (5.17), a generalization of this force can be shown to be given by

$$\mathbf{F}_\parallel = -\tfrac{1}{2}\frac{mv_\perp^2}{B}\nabla_\parallel B . \tag{5.72}$$

Thus a net force acts on charged particles–independent of their sign–in a direction opposite to that of increasing **B**.

5.8 Invariant of Motion

Constants of motion are important because they may reduce the number of independent variables in an equation characterizing some dynamic property of particles. In the absence of other force fields, the total energy E_o of a charged particle in a magnetic field is made up solely of the kinetic energy, since the only acting force, i.e. the Lorentz force, does not possess a potential energy; hence

$$E_o = \tfrac{1}{2}mv_\parallel^2 + \tfrac{1}{2}mv_\perp^2 \tag{5.73}$$

is a constant so that

$$\frac{d}{dt}\left(\tfrac{1}{2}mv_\parallel^2 + \tfrac{1}{2}mv_\perp^2\right) = 0 \tag{5.74}$$

where, as before, $v_\parallel$ and $v_\perp$ refer to velocity components parallel and perpendicular to the applied **B**-field direction.

Consider now the motion of a charged particle moving in a non-uniform **B**-field as described in the preceding section. Then, the parallel component of the force on this particle was seen to be given by the grad-B force, Eq. (5.72), as

$$\mathbf{F}_\parallel = m\frac{d\,\mathbf{v}_\parallel}{dt} = -\frac{mv_\perp^2}{2B}\frac{\partial \mathbf{B}}{\partial s} = -\mu\frac{\partial \mathbf{B}}{\partial s} \tag{5.75}$$

where ds is a differential path element along **B** and μ has been introduced representing the magnetic moment of the gyrating particle defined by

$$\mu = \frac{\tfrac{1}{2}mv_\perp^2}{B} . \tag{5.76}$$

Further, since $v_\parallel = ds/dt$, we write,

$$\frac{\partial \mathbf{B}}{\partial s} = \frac{\partial \mathbf{B}}{\partial s}\cdot\frac{ds}{dt}\cdot\frac{1}{v_\parallel} = \frac{1}{v_\parallel}\frac{d\mathbf{B}}{dt} \tag{5.77}$$

with (d**B**/dt) describing the variations of **B** as seen by the particle moving with speed $v_\parallel$. Combining this relation with Eq.(5.75) provides

$$m\frac{dv_\parallel}{dt} = -\frac{\mu}{v_\parallel}\frac{dB}{dt} \tag{5.78a}$$

or, respectively, in a rearranged form

$$\frac{d}{dt}\left(\tfrac{1}{2}mv_\parallel^2\right) = -\mu\frac{dB}{dt} . \tag{5.78b}$$

We now insert this relationship into Eq.(5.74) together with the definition of μ, Eq.(5.76), to obtain

$$\left[-\mu\frac{dB}{dt}\right] + \left[\frac{d}{dt}(\mu B)\right] = 0 . \tag{5.79}$$

Evidently, this relation holds only if

$$\frac{d}{dt}(\mu) = 0 \tag{5.80}$$

as the individual isolated charged particle moves in the spatially varying magnetic field. That is, the magnetic moment does not vary with time.

Note that the grad-B force of Eq. (5.72), used here for establishing Eq. (5.80), had been derived by approximating the radial magnetic field component according to Eq. (5.65). Hence, for the case considered, the magnetic moment μ is conserved only in this approximation. From the definition of μ, Eq. (5.76), it is evident that μ is an invariant if **B** is constant. For magnetic fields slowly varying in space and/or in time, that is, relative changes in B are very small over a distance equal to the radius of gyration,

$$\frac{r_g}{B}\nabla_\parallel B \ll 1 , \tag{5.81a}$$

and/or within a period of gyration,

$$\frac{1}{\omega_g B}\frac{dB}{dt} \ll 1 , \tag{5.81b}$$

the magnetic moment is found to remain invariant in this first-order approximation. Consequently, μ is only approximately conserved and therefore called an adiabatic invariant.

The practical consequence of this is as it relates to the so-called magnetic mirror effect. As **B** increases toward the "throat" of the mirror region, $v_\perp$ must increase and, in view of Eq.(5.74), $v_\parallel$ must decrease; thus, ions tend to decelerate along the axial direction as they move into the higher magnetic field of the mirror throat where $v_\perp$ can even become zero, if B is high enough. Note that $\mathbf{F}_\parallel$, which is given in Eq.(5.72) and which points opposite to ∇B, is still acting on the particles thus causing a reflection.

5.9 Cyclotron Radiation

We have established that the helical motion of a charged particle, guided by magnetic field lines as suggested in Fig. 5.5, involves a centripetal acceleration and therefore leads to the emission of radiation called cyclotron radiation and evidently involves an energy loss for the particle. We assess the associated power loss starting with the classical expression for the radiation emission rate of ions and electrons moving in an accelerating field which is known to exhibit the proportionality

$$P_{cyc} \propto N_i q_i^2 a_i^2 + N_e q_e^2 a_e^2 \approx N_e q_e^2 a_e^2 \tag{5.82}$$

where $a_{(\,)}$ denotes the respective accelerations and $q_{(\,)}$ the respective electrical charges with $q_i = |Zq_e|$. Here, the single particle radiation as given by Eq.(3.40) has been multiplied by the particle number density in order to provide an expression for power density. Note also that the smaller mass of the electrons will ensure that with their attendant higher acceleration–recall $a_e = F/m_e$–the electrons will be the predominant contributors to this cyclotron power loss. Ion cyclotron radiation is hence neglected. For cyclical motion in a magnetic field, the acceleration of electrons is a constant given by

$$a_e^2 = \left(\frac{v_{\perp e}^2}{r_{g,e}}\right)^2 = \left(\frac{v_{\perp e}^2}{r_{g,e}^2}\right) v_{\perp e}^2 . \tag{5.83}$$

Further, knowing the electron gyrofrequency as $\omega_{g,e} = |q_e|B/m_e$ with B as the controlling magnetic field, the relation of Eq. (5.41) allows us to write

$$\frac{v_{\perp e}^2}{r_{g,e}^2} = \frac{q_e^2 B^2}{m_e^2} . \tag{5.84}$$

Finally, assuming a Maxwellian distribution of electrons, we may take from kinetic energy considerations or Eq.(2.19b)

$$v_{\perp e}^2 \propto kT_e \tag{5.85}$$

giving therefore the cyclotron power density, Eq.(5.82) as,

$$P_{cyc} \propto N_e \left(\frac{q_e^4 B^2}{m_e^2}\right)(kT_e) \tag{5.86}$$

or

$$P_{cyc} = A_{cyc} N_e B^2 kT_e \tag{5.87}$$

where a constant of proportionality is explicitly introduced. With N_e in units of m^{-3}, B in units of Tesla, and kT in units of eV, the constant is given by $A_{cyc} \approx 6.3\times10^{-20}$ J·eV^{-1}· Tesla^{-2}·s^{-1} for P_{cyc} in units of W·m^{-3}. Thus, cyclotron radiation is most important at very high magnetic fields and high electron temperatures. Indeed, with electrons at a possibly very high energy, they may need to be subjected to a relativistic treatment.

Cyclotron radiation exists in the far infrared radiation spectrum with a wavelength of 10^{-3} - 10^{-4} m and is therefore partially re-absorbed in a plasma. Further, the emitted radiation may be reflected from the surrounding wall in a magnetic confinement fusion device and thereby re-enter the plasma. Hence, we choose to write the net cyclotron power finally lost from a plasma as

$$P_{cyc}^{net} = A_{cyc} N_e B^2 kT_e \psi \tag{5.88}$$

where ψ accounts for the complex processes of reflection and reabsorption of cyclotron radiation and is a dimensionless function involving several plasma parameters, including the magnetic field strength and the reflectivity of the surrounding wall. For a reasonable reflectivity of 90% and conditions expected in a fusion reactor, the range of ψ could typically be from 10^{-4} (for low T_e) to 10^{-2} (for very high T_e).

Problems

5.1 The maximum attainable magnetic field **B** is expected to be about 20 Tesla. For $v_{\parallel} \approx 0$, estimate the associated gyrofrequency, ω_g, and gyroradius, r_g, for electrons and protons given $kT_e = kT_i = 5$ keV.

5.2 Graphically depict the motion of an ion in a combined **E**-field and **B**-field. Display the results in an isometric representation.

5.3 (a) Determine the motion and position of a positive test charge in an electric field given by **E** = (E cos(ωt), 0, 0) with initial velocity **v**(0) = ($v_{x,o}$, 0, $v_{z,o}$) and initial position at the origin.

(b) For a similar positive test charge in only a magnetic field given by **B** = (B cos(ωt), 0, 0) with initial velocity **v**(0) = ($v_{x,o}$, $v_{y,o}$, $v_{z,o}$) and initial position at the origin, describe qualitatively and sketch the motion for $0 < t < 2\pi/\omega$ and $\omega << \omega_g$.

5.4 Perform the integration suggested in Eq.(5.49).

5.5 Confirm the statement in Sec. 5.6 that integrating the solution of Eq. (5.56c), given appropriate initial conditions, over one gyration period yields a drift in the negative-$v_{\parallel}$ direction dependent upon $v_{\perp}$.

5.6 As discussed at the end of Sec. 5.6, curvature drift and ∇B-drift will always occur together. Using the co-ordinate system of Fig. 5.10, approximate–in analogy to Sec. 5.5 and 5.6–the magnetic field strength **B**(y,z) = (0, B_y(y,z), B_z(y,z)) with a first order Taylor-expansion at the y-axis in order to account for both weak curvature and weak inhomogeneity (note that $\partial B_y/\partial y = \partial B_z/\partial z = 0$ at the reference point). What simple condition relating the degree of curvature an of inhomogeneity is then required to satisfy Maxwell's Eqs. (5.62) and (5.63)?

5.7 Demonstrate that the expression for the magnetic moment of an ion, Eq.(5.76), also follows from the basic definition of a current loop I encircling an area A (i.e., $\mu = IA$), and also identify the units for the magnetic moment μ.

5.8 Compare P_{cyc}^{net} with P_{br} for a deuterium-tritium plasma of density $N_e = N_i = 10^{20}$ m^{-3} confined by a magnetic field of magnitude B = 6 T.
Consider the specific cases:

(i) $T_e = 10$ keV; $\psi = 10^{-3}$
(ii) $T_e = 50$ keV; $\psi = 10^{-2}$

and also compare $P_{br} + P_{cyc}^{net}$ with P_{fu} at the given conditions.

5.9 Consider a 50:50% MCF device having $T_i = T_e$ and a plasma beta value of 0.2, and for which $\psi \approx 10^{-3}$. Compute and compare the modified ignition temperature, i.e. the temperature at which $P_{br} + P_{cyc}^{net} = f_{c,dt} P_{dt}$, to T^*_{ign} of problem 3.6.

5.10 Calculate an expression for the power density of cyclotron radiation emitted from a d-h fusion plasma of density $N_i + N_e$ and of kinetic temperature $T_i \approx T_e = T$ by knowing that a particle of charge q and velocity **v** will–according to classical electromagnetic theory–emit radiation at a power $P_{rad} \propto q^2 \, |\, d\mathbf{v}/dt \,|^2$.

(a) How much smaller is the cyclotron radiation power of ions than that of electrons?

(b) Compare the primary cyclotron radiation power density (that with no reabsorption) to the fusion energy release per unit time for the case of $N_d = N_h = 2 \times 10^{20}$ m^{-3}, T = 80 keV and B = 6 Tesla, and discuss the importance of radiation reflecting walls in an MCF reactor.

(c) Plot P_{cyc}^{net} (accounting for reflection and reabsorption by the approximation $\psi(T) \approx 10^{-4.2}$ [T(keV) / 1 keV]$^{1.4}$) and P_{br} as functions of T over the temperature range 10 to 120 keV.

6. Bulk Particle Transport

Media in which fusion reactions occur consist mainly of interspersed charged particles which are affected by short and long range forces. The cumulative effect of these forces combined with the intractability of an analytical description of each individual particle suggests that various approaches be used in the determination of the macroscopic behaviour of an ensemble of moving and colliding particles.

6.1 Particle Motion

The motion of a single particle of mass m is described by Newton's Law

$$m\frac{d\mathbf{v}}{dt} = \sum_j \mathbf{F}_j \tag{6.1}$$

where $\mathbf{F}_j$ is the j-th force vector acting on the particle and **v** is its velocity. For example, an isolated particle of mass m and charge q moving in a gravitational field **g**, an electric field **E**, and a magnetic field **B**, has its space-time trajectory described by

$$m\frac{d\mathbf{v}}{dt} = m\mathbf{g} + q\mathbf{E} + q(\mathbf{v} \times \mathbf{B}) . \tag{6.2}$$

While Eq.(6.2) is indeed very useful for some applications, it suffers from an overriding restriction: it describes the motion of an isolated particle only and thus excludes any possible interaction with other particles. This is indeed a severe restriction for fusion energy applications because power density requirements demand that about 10^{20} fusile ions be contained in one m^3; with such a large number of ions nearby each possessing a different velocity, it is evident that Coulomb interactions alone will lead to a most complex collection of time varying electrostatic forces acting on the particles. While in principle, one might specify a dynamical equation of the form of Eq.(6.1) for each particle, one would need perhaps 10^{20} force terms on the right hand side per unit volume; solving such equations for each of the interacting particles is, of course, totally unmanageable for computational purposes, due to the enormous number of these coupled equations and the lack of knowledge of individual initial conditions.

As an alternative to using an exceedingly large number of equations each containing many terms, it has been found that other approaches which are mathematically tractable provide, in selected applications, satisfactory agreement

with experiments and a useful predictive quality. One frequently used conceptual approach is to consider a plasma as a multicomponent interpenetrating low-density fluid and then employ suitable continuum mechanics methods. Another approach is to use probabilistic considerations for each group of particle species and then perform an analysis based on methods of sampling statistical physics.

While no one approach is generally applicable to all cases of conceivable interest, a careful choice of conceptual constructs and methodologies can lead to descriptions which are remarkably useful in characterizing selected space-velocity-time aspects of a particular species' population in a fusion medium. It is important therefore to develop a good understanding of the imposed assumptions in order to recognize important restrictions of a particular conceptual development and its consequent mathematical description.

6.2 Continuity and Diffusion

As a first fluidic description of a medium containing fusion fuel ions and sustaining fusion reactions, we consider a characterization which emphasizes particle mobility. Consider therefore an arbitrary volume V containing several time-varying particle populations $N_1^*(t)$, $N_2^*(t)$, ..., $N_j^*(t)$, ..., each species characterized by some macroscopic kinetic property such as temperature. We take the volume's surface to be non-reentrant and of total area A with its outward normal direction determined by the differential vector dA.

Our interest here is in the $N_j^*(t)$ population which, in the case of a spatially varying number density $N_j(\mathbf{r},t)$, is found from

$$N_j^*(t) = \int_V N_j(\mathbf{r},t)d^3r \ . \tag{6.3}$$

In general, the population $N_j^*(t)$ can change with time because of various types of gain and loss reaction rates, $R_{\pm j}^*$, and because of inflow and outflow rates, $F_{\pm j}^*$, across the total surface A. Hence, the rate equation for $N_j^*(t)$ is evidently

$$\frac{dN_j^*}{dt} = \left(\sum_k R_{+jk}^* - \sum_l R_{-jl}^*\right) + \left(F_{+j}^* - F_{-j}^*\right), \tag{6.4}$$

with the subscripts k and l enumerating different reaction types.

To begin, we now restrict ourselves to the case for which, in any fractional volume ΔV of V, the reaction contributions are zero or that the reaction gains are exactly canceled by the reaction losses; that is, we take

$$\sum_k R_{+jk}^* - \sum_l R_{-jl}^* = 0 \ . \tag{6.5}$$

Additionally, we refer to the condition

$$F_{+j}^* = 0 \tag{6.6}$$

which means there is no fueling by injection or other mechanisms, and we determine the outflow rate across the surface, accounting for global particle leakage, via the local particle current vector $\mathbf{J}_j(\mathbf{r},t)$ through

$$F_{-j}^* = \int_A \mathbf{J}_j(\mathbf{r},t)\cdot d\mathbf{A} \ . \tag{6.7}$$

As previously introduced, dA is an oriented surface element pointing outward. Obviously, particles leak out where $\mathbf{J}|_A$ also points in this outward direction.

We now substitute Eqs.(6.3) and (6.5) - (6.7) into Eq.(6.4) to obtain for the space-time description of the j-type particle species

$$\frac{d}{dt}\int_V N_j(\mathbf{r},t)d^3r = -\int_A \mathbf{J}_j(\mathbf{r},t)\cdot d\mathbf{A} \tag{6.8}$$

for the case specified by Eqs. (6.5) and (6.6). Then, in order to reduce both integrals to the same integration variable, we use Gauss' Divergence Theorem

$$\int_A \mathbf{J}_j(\mathbf{r},t)\cdot d\mathbf{A} = \int_V \nabla\cdot\mathbf{J}_j(\mathbf{r},t)d^3r \tag{6.9}$$

so that Eq.(6.8), with the inclusion of differentiation under the integral sign, becomes

$$\int_V \left[\frac{\partial}{\partial t}N_j(\mathbf{r},t) + \nabla\cdot\mathbf{J}_j(\mathbf{r},t)\right]d^3r = 0 \ . \tag{6.10a}$$

Here, the partial derivative is used since the temporal change in $N_j(\mathbf{r},t)$ is considered at fixed spatial coordinates, respectively. Since the volume V is arbitrary, we must therefore have

$$\frac{\partial}{\partial t}N_j(\mathbf{r},t) + \nabla\cdot\mathbf{J}_j(\mathbf{r},t) = 0 \ . \tag{6.10b}$$

This important relation is known as the Continuity Equation and must hold everywhere in the volume of interest and for all times of relevance providing the assumptions imposed here hold. If, however, there were sources and sinks for the considered species j in the volume of interest–i.e. reactions which produce or consume j-type particles–or particle injection, the corresponding gain and loss rate densities would appear on the right hand side of Eq.(6.10b).

Though compact, Eq.(6.10b) however suffers from a severe shortcoming: it represents only one equation containing two unknown functions, the scalar particle density $N_j(\mathbf{r},t)$ and the vector particle current $\mathbf{J}_j(\mathbf{r},t)$. Evidently, another relationship between these two quantities is necessary. As it turns out, this is often possible.

Many particle fluid media possess the property that the local particle current $\mathbf{J}(\mathbf{r},t)$ is proportional to the negative particle density gradient, $-\nabla N(\mathbf{r},t)$. This is often called a diffusion phenomenon and associated with the label Fick's Law. Introducing a proportionality factor D, called the diffusion coefficient, we may write therefore everywhere in the medium

with experiments and a useful predictive quality. One frequently used conceptual approach is to consider a plasma as a multicomponent interpenetrating low-density fluid and then employ suitable continuum mechanics methods. Another approach is to use probabilistic considerations for each group of particle species and then perform an analysis based on methods of sampling statistical physics.

While no one approach is generally applicable to all cases of conceivable interest, a careful choice of conceptual constructs and methodologies can lead to descriptions which are remarkably useful in characterizing selected space-velocity-time aspects of a particular species' population in a fusion medium. It is important therefore to develop a good understanding of the imposed assumptions in order to recognize important restrictions of a particular conceptual development and its consequent mathematical description.

6.2 Continuity and Diffusion

As a first fluidic description of a medium containing fusion fuel ions and sustaining fusion reactions, we consider a characterization which emphasizes particle mobility. Consider therefore an arbitrary volume V containing several time-varying particle populations $N_1^*(t)$, $N_2^*(t)$, ..., $N_j^*(t)$, ..., each species characterized by some macroscopic kinetic property such as temperature. We take the volume's surface to be non-reentrant and of total area A with its outward normal direction determined by the differential vector **dA**.

Our interest here is in the $N_j^*(t)$ population which, in the case of a spatially varying number density $N_j(\mathbf{r},t)$, is found from

$$N_j^*(t) = \int_V N_j(\mathbf{r},t)d^3r \ . \tag{6.3}$$

In general, the population $N_j^*(t)$ can change with time because of various types of gain and loss reaction rates, $R_{\pm j}^*$, and because of inflow and outflow rates, $F_{\pm j}^*$, across the total surface A. Hence, the rate equation for $N_j^*(t)$ is evidently

$$\frac{dN_j^*}{dt} = \left(\sum_k R_{+jk}^* - \sum_l R_{-jl}^*\right) + \left(F_{+j}^* - F_{-j}^*\right), \tag{6.4}$$

with the subscripts k and l enumerating different reaction types.

To begin, we now restrict ourselves to the case for which, in any fractional volume ΔV of V, the reaction contributions are zero or that the reaction gains are exactly canceled by the reaction losses; that is, we take

$$\sum_k R_{+jk}^* - \sum_l R_{-jl}^* = 0 \ . \tag{6.5}$$

Additionally, we refer to the condition

$$F_{+j}^* = 0 \tag{6.6}$$

which means there is no fueling by injection or other mechanisms, and we determine the outflow rate across the surface, accounting for global particle leakage, via the local particle current vector $\mathbf{J}_j(\mathbf{r},t)$ through

$$F_{-j}^* = \int_A \mathbf{J}_j(\mathbf{r},t)\cdot d\mathbf{A} \ . \tag{6.7}$$

As previously introduced, dA is an oriented surface element pointing outward. Obviously, particles leak out where $\mathbf{J}|_A$ also points in this outward direction.

We now substitute Eqs.(6.3) and (6.5) - (6.7) into Eq.(6.4) to obtain for the space-time description of the j-type particle species

$$\frac{d}{dt}\int_V N_j(\mathbf{r},t)d^3r = -\int_A \mathbf{J}_j(\mathbf{r},t)\cdot d\mathbf{A} \tag{6.8}$$

for the case specified by Eqs. (6.5) and (6.6). Then, in order to reduce both integrals to the same integration variable, we use Gauss' Divergence Theorem

$$\int_A \mathbf{J}_j(\mathbf{r},t)\cdot d\mathbf{A} = \int_V \nabla\cdot\mathbf{J}_j(\mathbf{r},t)d^3r \tag{6.9}$$

so that Eq.(6.8), with the inclusion of differentiation under the integral sign, becomes

$$\int_V \left[\frac{\partial}{\partial t}N_j(\mathbf{r},t) + \nabla\cdot\mathbf{J}_j(\mathbf{r},t)\right]d^3r = 0 \ . \tag{6.10a}$$

Here, the partial derivative is used since the temporal change in $N_j(\mathbf{r},t)$ is considered at fixed spatial coordinates, respectively. Since the volume V is arbitrary, we must therefore have

$$\frac{\partial}{\partial t}N_j(\mathbf{r},t) + \nabla\cdot\mathbf{J}_j(\mathbf{r},t) = 0 \ . \tag{6.10b}$$

This important relation is known as the Continuity Equation and must hold everywhere in the volume of interest and for all times of relevance providing the assumptions imposed here hold. If, however, there were sources and sinks for the considered species j in the volume of interest–i.e. reactions which produce or consume j-type particles–or particle injection, the corresponding gain and loss rate densities would appear on the right hand side of Eq.(6.10b).

Though compact, Eq.(6.10b) however suffers from a severe shortcoming: it represents only one equation containing two unknown functions, the scalar particle density $N_j(\mathbf{r},t)$ and the vector particle current $\mathbf{J}_j(\mathbf{r},t)$. Evidently, another relationship between these two quantities is necessary. As it turns out, this is often possible.

Many particle fluid media possess the property that the local particle current $\mathbf{J}(\mathbf{r},t)$ is proportional to the negative particle density gradient, $-\nabla N(\mathbf{r},t)$. This is often called a diffusion phenomenon and associated with the label Fick's Law. Introducing a proportionality factor D, called the diffusion coefficient, we may write therefore everywhere in the medium

$$\mathbf{J}_j(\mathbf{r},t) = -D_j \nabla N_j(\mathbf{r},t) \tag{6.11}$$

so that, by substitution into Eq.(6.10b) we get

$$\frac{\partial}{\partial t} N_j(\mathbf{r},t) + \nabla \cdot \left[- D_j \nabla N_j(\mathbf{r},t) \right] = 0 . \tag{6.12}$$

Numerous reductions are now often applicable. If the medium is homogeneous and isotropic then the diffusion coefficient is a space-independent scalar, and we obtain

$$\frac{\partial}{\partial t} N_j(\mathbf{r},t) - D_j \nabla^2 N_j(\mathbf{r},t) = 0 . \tag{6.13}$$

Steady-state conditions in such a medium will yield Laplace's Equation

$$\nabla^2 N_j(\mathbf{r},t) = 0 . \tag{6.14}$$

The diffusion coefficient in Eq.(6.12), D_j, is clearly of importance in specifying the spatial variation of the particle density $N_j(\mathbf{r},t)$. Considerable thought has gone into analytical characterizations of this parameter so that the diffusion processes be adequately incorporated. For example, for neutral particles in random thermal motion and in regions sufficiently far from boundaries, it has been found that, to a good approximation

$$D_j \propto \bar{v}_j \lambda_j \tag{6.15}$$

where $\bar{v}_j$ is the mean speed of the j-type particles and λ_j is the mean-free-path between scattering collisions among the j-type particles–and is much smaller than $(\nabla N/N)^{-1}$.

In contrast to neutral particles, charged particle motion in a magnetic field may involve considerable anisotropic diffusion governed by the local **B**-field requiring that a distinction between a direction which is parallel or perpendicular to the local **B**-field be made. Relationships with a good physical basis in classical diffusion are

$$D_\parallel \propto \left(\bar{v}\right)^2 \tau_c \tag{6.16a}$$

$$D_\perp \propto \frac{\left(\bar{v}\right)^2}{\omega_g^2 \tau_c} , \tag{6.16b}$$

where ω_g is the gyrofrequency and τ_c is the mean collision time.

By analogy to the mean-time between fusion events τ_{fu}, Eq.(4.3), we take herein

$$\tau_c \propto \frac{1}{\sigma_s v} \propto v^3 \tag{6.17}$$

and recall that the Coulomb cross section σ_s varies as v^{-4}, Eq.(3.15).

Further, substituting for the averaged square velocity by the thermal energy $E_{th} \propto kT$, or the kinetic temperature, respectively, and using the explicit

expression for ω_g given in Eq.(5.12), we rewrite Eq.(6.16a) and (6.16b) to exhibit the proportionalities

$$D_\parallel \propto T^{5/2} \tag{6.18a}$$

and

$$D_\perp \propto \frac{1}{B^2 \sqrt{T}} . \tag{6.18b}$$

Thus, a higher temperature and an increasing magnetic field will reduce classical diffusion across the **B**-field lines. This conclusion must, however, be tempered by the recognition that collective oscillations in a plasma destroy some of the classical diffusion features. The plasmas of interest to nuclear fusion applications are severely affected by such collective processes through plasma instabilities which do not obey classical diffusion considerations.

The destabilizing oscillations induce turbulent phenomena which enhance diffusion across the magnetic field lines. Incorporation of these considerations leads to so-called Bohm diffusion characterized by

$$D_B \propto \frac{T}{B} \tag{6.19}$$

thereby placing greater demands on magnetic confinement at higher temperature.

Finally, we add that the Continuity Equation for the particle density $N_j(\mathbf{r},t)$, Eq.(6.13), translates into an equation for the mass density ρ_j by using $\rho_j(\mathbf{r},t) = N_j(\mathbf{r},t)m_j$,

$$\frac{\partial}{\partial t} \rho_j(\mathbf{r},t) - D_j \nabla^2 \rho_j(\mathbf{r},t) = 0 \tag{6.20}$$

and is generally found to be of considerable utility, particularly in conjunction with other relationships as we will show next.

6.3 Particle-Fluid Connection

The preceding analysis leads to a compact space-time description for the particle or mass density. Of particular interest to us now is a characterization of collective motion in a plasma. In such a description, the identity of individual particles is put aside and the plasma is characterized by the space-time changes of macroscopic variables such as bulk speed, temperature, and pressure defined in a fluidic context.

To begin with we take the Continuity Equation, Eq.(6.12), as a necessary equation for the particle density everywhere in space and time. That is, if another equation is developed in which $N_j(\mathbf{r},t)$ appears as an independent function, both equations must hold simultaneously and any solution methodology is expected to involve both equations.

To be specific, we consider a space-time ensemble of N_j particles each of

mass m_j and charge q_j to which we assign an average velocity $\mathbf{V}_j$ over an infinitesimal volume containing N_j. A simplified one-dimensional analogy is the case of freeway traffic with cars moving at different speeds, all together amounting to some average speed of traffic motion which, nonetheless, may vary with time and location.

In order to provide some continuity to our preceding analysis, we suppose that an electric field **E** and magnetic field **B** act on this moving space-time ensemble of N_j particles, referred to as a fluid element. Its equation of motion is

$$N_j m_j \frac{d\mathbf{V}_j}{dt} = N_j q_j \mathbf{E} + N_j q_j (\mathbf{V}_j \times \mathbf{B}), \quad j = i,e . \tag{6.21}$$

Recall that N_j used here is determined by Eq.(6.12) everywhere in space and time.

Imposing our space-time variation on the ensemble-average-velocity we specify $\mathbf{V}_j$ as a function of space and time, that is

$$\mathbf{V}_j(\mathbf{r},t) = \mathbf{V}_j(x,y,z,t) . \tag{6.22}$$

Performing the differentiation in Eq.(6.21), according to the chain rule gives specifically

$$\frac{d\mathbf{V}_j}{dt} = \frac{\partial \mathbf{V}_j}{\partial x}\frac{dx}{dt} + \frac{\partial \mathbf{V}_j}{\partial y}\frac{dy}{dt} + \frac{\partial \mathbf{V}_j}{\partial z}\frac{dz}{dt} + \frac{\partial \mathbf{V}_j}{\partial t} \tag{6.23a}$$

or, in more compact vector notation

$$\frac{d\mathbf{V}_j}{dt} = (\mathbf{V}_j \cdot \nabla)\mathbf{V}_j + \frac{\partial \mathbf{V}_j}{\partial t} . \tag{6.23b}$$

The two terms on the right hand side possess an easily established interpretation; clearly, the second term $\partial \mathbf{V}_j/\partial t$ is simply the acceleration of the N_j ensemble at a fixed coordinate point; then, the first term incorporates the process of spatial variation in the ensemble velocity much as in our one-dimensional analogy the traffic in one section of the freeway may move faster than that in another section; the term convection is often used for this kind of fluid motion. We insert Eq.(6.23b) into Eq.(6.21) and again use $\rho_j = N_j m_j$ to obtain a corresponding equation for the ensemble's motion

$$\rho_j \left[(\mathbf{V}_j \cdot \nabla)\mathbf{V}_j + \frac{\partial \mathbf{V}_j}{\partial t} \right] = \rho_j^c \mathbf{E} + \rho_j^c (\mathbf{V}_j \times \mathbf{B}) \tag{6.24}$$

where the mass density ρ_j satisfies the Continuity Equation, Eq.(6.20), and $\rho_j^c(\mathbf{r},t) = N_j(\mathbf{r},t)q_j$ is the respective charge density. Note that, because of electromagnetic interactions in a plasma, ρ_j^c, **E** and **B** are all related via Maxwell's Equation which, simultaneously, must also hold with Eq.(6.24).

At this juncture, we recognize another process which is generally important in a hot plasma: the thermal motion of particles makes them randomly enter and exit the fluid element considered, leading to local pressure gradients which act as an additional force in Eq.(6.24). While, in general, this force can be obtained

from the divergence of a stress tensor, we consider here the case of an isotropic fluid, for which we add the term $-\nabla p_j$ to Eq.(6.24) in order to include this force effect; finally then, the motion of a fluid element is given by

$$\rho_j \left[(\mathbf{V}_j \cdot \nabla)\mathbf{V}_j + \frac{\partial \mathbf{V}_j}{\partial t} \right] = \rho_j^c \mathbf{E} + \rho_j^c (\mathbf{V}_j \times \mathbf{B}) - \nabla p_j \tag{6.25}$$

wherein the local particle pressures are related to the respective mass density via the Equation of State

$$p_j = C \rho_j^{\gamma_j} \tag{6.26}$$

where C is a constant and γ_j is the ratio of specific heats for constant pressure and constant volume ($\gamma_j = C_p/C_V$) referring to the j-th species.

An important point must be emphasized that concerns the electric and magnetic fields, **E** and **B**, when the above set of equations is evaluated for ions and electrons. As noted previously, it is required that Maxwell's Equations be satisfied for the medium of interest. The complete set of resultant equations for ρ_i, ρ_e, $\mathbf{V}_i$, $\mathbf{V}_e$, p_i, p_e, **E**, **B**–consisting of 16 simultaneous scalar equations–represents what is known as a self-consistent description of the plasma fluid approximation by the so called magnetohydrodynamic (MHD) equations. The imposition of initial and boundary conditions clearly leads to a nontrivial problem description.

6.4 Particle Kinetic Description

As a final characterization of a statistically varying population, we consider what is often called transport theory or a kinetic description. A compact derivation which leads to a defining equation for a particle density distribution function and which also includes collisional effects as well as source effects–that is, comprehensive transport of particles and their properties–is suggested in the following.

Consider an ensemble of N particles each characterized by a distinguishable velocity vector $\mathbf{v}_i$ and coordinate vector $\mathbf{r}_i$ at time t. For that we introduce a distribution function f_N represented by

$$f_N = f_N(\mathbf{r}_1, \mathbf{v}_1; \mathbf{r}_2, \mathbf{v}_2; \ldots; \mathbf{r}_i, \mathbf{v}_i; \ldots; \mathbf{r}_N, \mathbf{v}_N; t), \tag{6.27}$$

which is able to specify the probability that at time t, the particle 1 is found about the coordinate $\mathbf{r}_1$ with the velocity vector $\mathbf{v}_1$ while the position and velocity of particle 2 are about $\mathbf{r}_2$ and $\mathbf{v}_2$, and the remaining (N-2) particles are similarly found at distinct coordinate intervals in the position-velocity space. With N as the number of particles of interest, each characterized by three Cartesian space coordinates and three Cartesian velocity components, this phase-space is evidently a 6N-dimensional phase-space.

A fundamental principle in the description of particle distributions is known

as the Liouville Theorem; this theorem states that a volume element in the 6N-dimensional phase-space remains constant for the motion of particles obeying the Hamiltonian equation of motion. For the N-particle distribution function f_N, Eq.(6.27), this theorem leads to the Liouville Equation

$$\frac{df_N}{dt} = 0 \tag{6.28}$$

if particle creation and/or particle destruction does not occur. Performing the differentiation of Eq.(6.28), the explicit differentiation which f_N must satisfy is evidently

$$\left[\frac{\partial}{\partial t} + \sum_{i=1}^{N}\left(\mathbf{v}_i \cdot \frac{\partial}{\partial \mathbf{r}_i} + \frac{d\,\mathbf{v}_i}{dt}\frac{\partial}{\partial \mathbf{v}_i}\right)\right] f_N = 0\,. \tag{6.29}$$

This differential equation is generally the starting point for an analysis of a many particle system. Note that the acceleration term $d\mathbf{v}_i/dt$ can be replaced by $\mathbf{F}_i/m_i$ via Newton's Law with $\mathbf{F}_i$ representing the total force acting on the i-th particle.

Equation (6.29) is now subject to integration over a suitable large set of coordinates $\mathbf{r}_i$ and velocities $\mathbf{v}_i$ in order to substantially reduce the dimensionality of the phase-space distribution function from f_N to, say f_r. Thus, for $r << N$, we obtain

$$f_r(\mathbf{r}_1, \mathbf{v}_1; \ldots; \mathbf{r}_r, \mathbf{v}_r; t) = A_r \int f_N \prod_{i=r+1}^{N} d^3 r_i\, d^3 \mathrm{v}_i \tag{6.30}$$

with A_r a normalization constant generally chosen by convention, e.g. $A_r = 1/(N - r)!$, found via permutational calculus.

We will find it useful to separate the total force $\mathbf{F}_i$ acting on the i-th particle into its internal (inter-particle) and external components, $\sum_{j=1}^{N} \mathbf{F}_{ij}$ and $\mathbf{F}_i^{ext}$. Further, assuming that f_N vanishes on the boundaries of the phase space and that the only velocity-dependent forces are of Lorentzian form as in Eq.(5.6), the integration of Eq.(6.29) over the $6(N - r)$ variables $\mathbf{r}_{r+1},\ldots,\mathbf{r}_N,\mathbf{v}_{r+1},\ldots,\mathbf{v}_N$ leads–in combination with Eq.(6.30) and using the normalization of A_r–to

$$\left[\frac{\partial}{\partial t} + \sum_{i=1}^{r}\left(\mathbf{v}_i \cdot \nabla_{r_i} + \frac{\mathbf{F}_i^{ext} + \sum_{j=1}^{r}\mathbf{F}_{ij}}{m_i} \cdot \nabla_{\mathrm{v}_i}\right)\right] f_r = -\sum_{i=1}^{r}\frac{1}{m_i}\int \mathbf{F}_{i,r+1} \cdot \nabla_{\mathrm{v}_i} f_{r+1}\, d^3 \mathrm{r}_{r+1}\, d^3 \mathrm{v}_{r+1}$$

$$\mathrm{j} \neq \mathrm{i}\,, \quad \mathrm{r} = 1, 2, \ldots, \mathrm{N} - 1\,, \tag{6.31a}$$

where we replaced $\partial/\partial\mathbf{r}$ and $\partial/\partial\mathbf{v}$ by the gradient symbols

$$\nabla_r = \frac{\partial}{\partial x}\mathbf{i} + \frac{\partial}{\partial y}\mathbf{j} + \frac{\partial}{\partial z}\mathbf{k} \tag{6.31b}$$

and

$$\nabla_{\mathrm{v}} = \frac{\partial}{\partial \mathrm{v}_x}\mathbf{i} + \frac{\partial}{\partial \mathrm{v}_y}\mathbf{j} + \frac{\partial}{\partial \mathrm{v}_z}\mathbf{k}\,. \tag{6.31c}$$

Equation (6.31a) is known as the Bogolyubov-Born-Green-Kirkwood-Yvon hierarchy and closes only with the Liouville Equation, Eq.(6.28), since the equation for f_r contains f_{r+1}. To accommodate the cutting off of this sequence at a reasonably small r, a physical approximation for f_{r+1} is therefore needed in terms of $f_1,\ldots,f_r$ in order to arrive at a solvable set of equations. From this set of r equations the r-1 equations may be used to eliminate $f_2,\ldots,f_r$, leaving a single kinetic equation for the one-particle distribution function f_1.

We now consider the case r = 1 which is described by

$$\frac{\partial f_1}{\partial t} + \mathbf{v}_1 \cdot \nabla_{r_1} f_1 + \frac{\mathbf{F}_1^{ext}}{m_1} \cdot \nabla_{\mathrm{v}_1} f_1 = -\frac{1}{m_1}\int \mathbf{F}_{12} \cdot \nabla_{\mathrm{v}_1} f_2\, d^3 r_2\, d^3 \mathrm{v}_2\,. \tag{6.32}$$

Here, $f_1(\mathbf{r}_1,\mathbf{v}_1,t)$ is the one-particle distribution function used to determine the probability of finding particle 1 at time t about the position $\mathbf{r}_1$ with velocity $\mathbf{v}_1$; note however, that herein we have lost the corresponding information about the other particles. Further, Eq.(6.32) contains the two-particle distribution $f_2(\mathbf{r}_1,\mathbf{v}_1,\mathbf{r}_2,\mathbf{v}_2,t)$ which specifies the probability that at time t particle 1 moves with $\mathbf{v}_1$ about $\mathbf{r}_1$ and, simultaneously, particle 2 will be found about $\mathbf{r}_2$ with velocity $\mathbf{v}_2$, with no such individual information about the remaining N-2 particles.

Writing the one-particle distributions

$$f_1(\mathbf{r}_1, \mathbf{v}_1, t) = f(1) \tag{6.33a}$$

for particle 1,

$$f_1(\mathbf{r}_2, \mathbf{v}_2, t) = f(2) \tag{6.33b}$$

for particle 2, and expressing the two-particle distribution by cluster expansion as

$$f_2(\mathbf{r}_1, \mathbf{v}_1, \mathbf{r}_2, \mathbf{v}_2, t) = f(1)f(2) + C(1,2) \tag{6.33c}$$

with C representing the so-called pair correlation function relating kinetic variations of particles 1 and 2, most significantly within the close range of their interaction, we find upon substitution of these expansions the following kinetic equation:

$$\frac{\partial f(1)}{\partial t} + \mathbf{v}_1 \cdot \nabla_{r_1} f(1) + \frac{\mathbf{F}_1^{ext}}{m_1} \cdot \nabla_{\mathrm{v}_1} f(1) + \frac{1}{m_1}\left(\int \mathbf{F}_{12} f(2)\, d^3 r_2\, d^3 \mathrm{v}_2\right) \cdot \nabla_{\mathrm{v}_1} f(1)$$
$$= -\frac{1}{m_1}\int \mathbf{F}_{12} \cdot \nabla_{\mathrm{v}_1} C(1,2)\, d^3 r_2\, d^3 \mathrm{v}_2\,. \tag{6.34}$$

The expression within brackets in the fourth term on the left-hand side represents the field force experienced by particle one due to the presence of the other particles and may be written as

$$\int \mathbf{F}_{12} f(2)\, d^3 r_2\, d^3 \mathrm{v}_2 = \mathbf{F}_1^{field}\,. \tag{6.35}$$

Actually, this is the particle contribution to the self-consistent field (for example:

an ion distribution generates an electromagnetic field which in turn maintains this distribution).

The right-hand side of Eq.(6.34) is the collision term for which some approximation must be applied to expand it also as a function of f(1) and f(2). Since various physical models exist for approximating the collision term, we choose to represent it here simply by $(\partial f(1)/\partial t)_c$. Thus the final kinetic equation for a one-particle distribution function is

$$\frac{\partial}{\partial t} f(\mathbf{r},\mathbf{v},t) + \mathbf{v}\cdot\nabla_r f + \frac{\mathbf{F}}{m}\cdot\nabla_v f = \left(\frac{\partial f}{\partial t}\right)_c \tag{6.36}$$

where **F** includes all external and field forces. Herein and subsequently we omit the subscript and f(**r**,**v**,t) will refer to the one-particle distribution function which is representative of any one of the considered N particles of the same species, however does not provide information which distinguishes the individual kinetic behaviour of the particles. For charged particles moving in an electric and magnetic field, the total force is evidently

$$\mathbf{F} = q(\mathbf{E} + \mathbf{v}\times\mathbf{B}) \tag{6.37}$$

incorporating self-consistent fields.

If particle production and/or destruction also take place and particles can leave and/or enter the reaction volume under consideration, then we account for these sources and sink processes on the right-hand side of Eq.(6.36) by an additional term $(\partial f/\partial t)_s$ to be specified according to the appropriate conditions.

In the statistical sense [f(**r**,**v**,t) d^3r d^3v] is interpreted as the probability of finding at time t a particle of the species of interest in the differential volume element d^3r d^3v about the point (**r**,**v**) in the 6-dimensional phase space, Fig.6.1. We may now conclude that the expected number of such particles in this differential volume element is

$$N(\mathbf{r},\mathbf{v},t)d^3r\,d^3v = N^* f(\mathbf{r},\mathbf{v},t)d^3r\,d^3v \tag{6.38}$$

where N^* is the total number of particles in the entire volume at some reference time. Hence

$$N(\mathbf{r},\mathbf{v},t)d^3r\,d^3v = \begin{pmatrix}\text{expected number of particles in } d\mathbf{r}\\ \text{about } \mathbf{r} \text{ and in } d\mathbf{v} \text{ about } \mathbf{v} \text{ at time t}\end{pmatrix}. \tag{6.39}$$

Obviously the normalization applied to Eq.(6.39) is

$$\iint f(\mathbf{r},\mathbf{v},t)d^3r\,d^3v = \frac{N(t)}{N^*} \tag{6.40}$$

with the number density obtained by

$$N(\mathbf{r},t) = \int N(\mathbf{r},\mathbf{v},t)d^3v = N^*\int f(\mathbf{r},\mathbf{v},t)d^3v\,. \tag{6.41}$$

The transport equation for a charged particle density distribution N(**r**,**v**,t) in an electric and magnetic field and subjected to collisional effects as well as to particle production/destruction is therefore finally written as

$$\frac{\partial N}{\partial t} + \mathbf{v}\cdot\nabla_r N + \frac{q}{m}(\mathbf{E}+\mathbf{v}\times\mathbf{B})\cdot\nabla_v N = \left(\frac{\partial N}{\partial t}\right)_c + \left(\frac{\partial N}{\partial t}\right)_s\,. \tag{6.42}$$

A solution analysis of this equation for N = N(**r**,**v**,t) requires the self-consistent specification of **E** and **B** (determined in conjunction with Maxwell's Equations) everywhere, identification of the form of the collision and source/sink terms and the imposition of initial and boundary conditions. A reaction domain will generally contain more than one species of particles so that the determination of the overall collision kinetics requires several equations of the form of Eq.(6.42)–one for each species. All of these may be coupled by several collision terms since collisions will invariably occur among the same and other species. Needless to say, the dimensionality of this problem is formidable. A simplification is possible by a reduction of the number of independent variables and elimination of some terms depending upon the problem of interest.

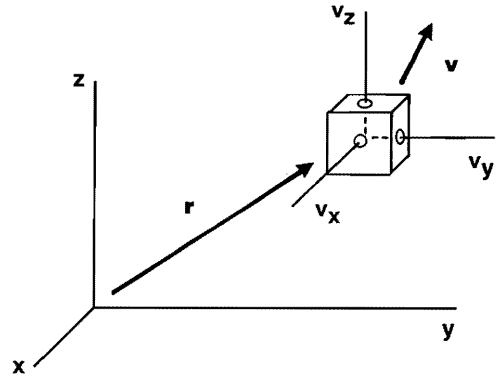

Fig. 6.1: Depiction of a 6-dimensional coordinate-velocity phase space volume element.

It is useful to note that the left-hand side of Eq.(6.42) constitutes, by our classification of processes, continuous changes in phase space while the right-hand parts are discontinuous changes. Thus, particle collisions, particle reactions and particle destructions are viewed as discontinuous–that is discrete processes–whereas particle acceleration can vary smoothly in the coordinate-velocity space. If only binary collisions are considered, the analysis is labeled "classical" or "neoclassical" if applied to toroidal geometry. As plasma wave-particle interactions become dominant such that the transport of mass, momentum or energy results therefrom, then the label "anomalous transport" is used.

6.5 Global Particle Leakage

In addition to the particle-fluid characterization of a plasma, one may identify probabilistic methodologies which, in selected applications are most useful. We discuss here one such approach to the assessment of particle leakage from a fusion reaction volume.

Consider a volume V containing $N^*_j(t)$ particles of the j-type. This population changes with time because of gain and loss reaction rates, R^*_{+j} and R^*_{-j}, respectively, and also because of particle injection and leakage rates, F^*_{+j} and F^*_{-j}, Fig.6.2. The rate equation is evidently

$$\frac{dN^*_j}{dt} = \left(R^*_{+j} - R^*_{-j}\right) + \left(F^*_{+j} - F^*_{-j}\right). \tag{6.43}$$

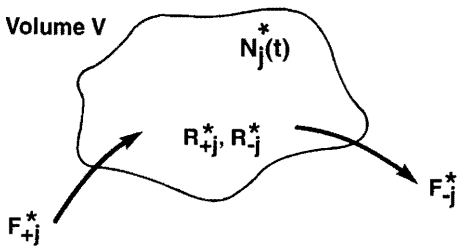

Fig. 6.2: Volume V containing population $N^*_j(t)$ which is subjected to gain and loss reaction rates, R^*_{+j} and R^*_{-j}, as well as particle injection and leakage rates, F^*_{+j} and F^*_{-j}.

Our interest is specifically in the particle leakage rate F^*_{-j} and we wish to explore an approach which has no need for a detailed space distribution of the particle population; that is, we consider a probabilistic formulation in an integrated global sense for this arbitrary volume.

As our underlying physical basis, we adopt the proposition that the statistically expected fractional change in the population due to particle leakage is $-\Delta N^*_j/N^*_j$ in an interval of time Δt, and is only a function of time. This statement can be expressed in algebraic form as

$$-\left[\frac{\Delta N^*_j / N^*_j}{\Delta t}\right]_{leakage} = \lambda_j(t), \tag{6.44a}$$

where $\lambda_j(t)$ is a positive function of time to be considered subsequently. For now, we take the limit of $\Delta t \rightarrow dt$ to write

$$-\left[\frac{1}{N^*_j}\frac{dN^*_j}{dt}\right]_{leakage} = \lambda_j(t). \tag{6.44b}$$

Hence for an initial population $N^*_j(0)$, the fraction of particles remaining up to time t–that is the non-leakage fraction–follows by integration and gives

$$\left[\frac{N^*_j(t)}{N^*_j(0)}\right]_{non\text{-}leakage} = exp\left[-\int_0^t \lambda_j(t')dt'\right]. \tag{6.45}$$

A re-examination of Eq.(6.44b) provides us with a useful expression if we recall that

$$F^*_{-j} = \left|\left[\frac{dN^*_j}{dt}\right]_{leakage}\right| \tag{6.46}$$

and therefore

$$F^*_{-j} = \lambda_j(t)\, N^*_j(t). \tag{6.47}$$

However, this expression tells us little about the meaning of $\lambda_j(t)$ nor does it provide a suggestion on how to calculate it. This can be resolved if we introduce some probabilistic considerations.

Consider the probability density function $f_j(t)$ which describes the outcome that a particle j remains in the volume V over a time t until it escapes from the ensemble. Hence, this probability is given by the product of the following probabilities which also define $f_j(t)$:

$$f_j(t)dt = \begin{bmatrix}\text{probability of}\\ \text{non - leakage}\\ \text{until time t}\end{bmatrix}\begin{bmatrix}\text{probability of}\\ \text{leakage during}\\ \text{time dt}\end{bmatrix}$$

$$= \left[exp\left(-\int_0^t \lambda_j(t')dt'\right)\right]\left[\left[\frac{|dN^*_j|}{N^*_j}\right]_{dt}\right] \tag{6.48}$$

$$= \left[exp\left(-\int_0^t \lambda_j(t')dt'\right)\right]\left[\lambda_j(t)dt\right].$$

Note that the substitution here follows directly from Eq.(6.44). Thus, the probability density function of interest is evidently

$$f_j(t) = \lambda_j(t)\, exp\left(-\int_0^t \lambda_j(t')dt'\right). \tag{6.49}$$

with the normalization $\int_0^\infty f_j(t)dt = 1$ as required.

With $f_j(t)$ now specified, we may compute some interesting time dependent quantities. Of particular interest is the particle mean residence time until leakage. Using τ^*_j for this quantity, we may compute it as

$$\tau_j^* = \int_0^\infty t\, f_j(t)\, dt = \int_0^\infty t \left[\lambda_j(t)\, exp\left(- \int_0^\infty \lambda_j(t')dt' \right) \right] dt \,. \qquad (6.50)$$

If the statistical leakage fraction per unit time, Eq.(6.44a), is a constant, then $\lambda_j(t) \rightarrow \lambda_j$ and Eq.(6.50) can be integrated to yield

$$\tau_j^* = \int_0^\infty t\, \lambda_j\, exp(-\lambda_j t) dt = \frac{1}{\lambda_j} \,. \qquad (6.51)$$

That is, λ_j is the inverse mean residence time of the particle in the volume of interest and a more self-explanatory expression for the leakage rate is therefore

$$F_{-j}^* = \frac{N_j^*(t)}{\tau_j^*} \qquad (6.52)$$

where in the context of nuclear fusion, τ_j^* is often called the global particle leakage or confinement time. A good estimate of τ_j^* can frequently be obtained from a knowledge of the mean particle speed and the mean cumulative distance a particle travels in a reaction volume.

We add that by a similar derivational development, one may show that the energy leakage rate–that is power leakage–from a fusion reaction volume is given by

$$P_-^* = \frac{E^*(t)}{\tau_{E^*}} \qquad (6.53)$$

where $E^*(t)$ is the total energy content of the reaction volume and τ_{E^*} is the global mean energy leakage time or global energy confinement time.

Problems

6.1 Specify the conditions which reduce Eq.(6.21) to its simplest form while still retaining electric and magnetic field effects.

6.2 Consider a particle density N(x, y, z, E, θ, ϕ) and formulate a reduced transport equation, Eq.(6.42), for each of the following cases:

(a) neutral particles,
(b) monoenergetic particles,
(c) only the z-direction is relevant, and
(d) both the source and collision terms are given.

6.3 Consider a plasma contained between two walls x_0 units apart and effectively infinite in the y and z-directions. For the case that the plasma decays by diffusion to the walls and for separability of the form $N(\mathbf{r},t) = R(\mathbf{r})\, T(t)$, determine $N(\mathbf{r},t)$ throughout this plasma slab region for all time. Sketch this density function.

6.4 Confirm that for a cylindrically-shaped, magnetically confined plasma wherein radial diffusion is the dominant mode of transport, assuming a constant volumetric ion source, the steady state ion density will have the following relationship:

$$N(r) = N(0)\sqrt{1 - \frac{r^2}{a^2}} \,, \qquad (6.54)$$

where N(0) is the ion density at r = 0, and a is the plasma minor radius. (Note that for these conditions, Eq.(6.10b) becomes $\nabla \times \mathbf{J}(\mathbf{r}) = S$ = constant.)

6.5 Given Eq.(6.54) for the ion density radial distribution, derive the average ion density.